Accepted Manuscript

Design, synthesis and biological evaluation of *N*-((1-benzyl-1*H*-1,2,3-triazol-4-yl)methyl)-1,3-diphenyl-1*H*-pyrazole-4-carboxamides as CDK1/Cdc2 inhibitors

V. Ganga Reddy, T. Srinivasa Reddy, V. Lakshma Nayak, Budaganaboyina Prasad, Adiyala Praveen Reddy, A. Ravikumar, Shaik Taj, Ahmed Kamal

PII: S0223-5234(16)30488-3

DOI: 10.1016/j.ejmech.2016.06.011

Reference: EJMECH 8672

To appear in: *European Journal of Medicinal Chemistry*

Received Date: 16 March 2016

Revised Date: 5 June 2016

Accepted Date: 8 June 2016

Please cite this article as: V. Ganga Reddy, T. Srinivasa Reddy, V. Lakshma Nayak, B. Prasad, A.P. Reddy, A. Ravikumar, S. Taj, A. Kamal, Design, synthesis and biological evaluation of *N*-((1-benzyl-1*H*-1,2,3-triazol-4-yl)methyl)-1,3-diphenyl-1*H*-pyrazole-4-carboxamides as CDK1/Cdc2 inhibitors, *European Journal of Medicinal Chemistry* (2016), doi: 10.1016/j.ejmech.2016.06.011.

Graphical Abstract

Design, synthesis and biological evaluation of *N*-((1-benzyl-1*H*-1,2,3-triazol-4-yl)methyl)-1,3-diphenyl-1*H*-pyrazole-4-carboxamides as CDK1/Cdc2 inhibitors

V. Ganga Reddy, T. Srinivasa Reddy, V. Lakshma Nayak, Budaganaboyina Prasad, Adiyala Praveen Reddy, A. Ravikumar, Shaik Taj, Ahmed Kamal

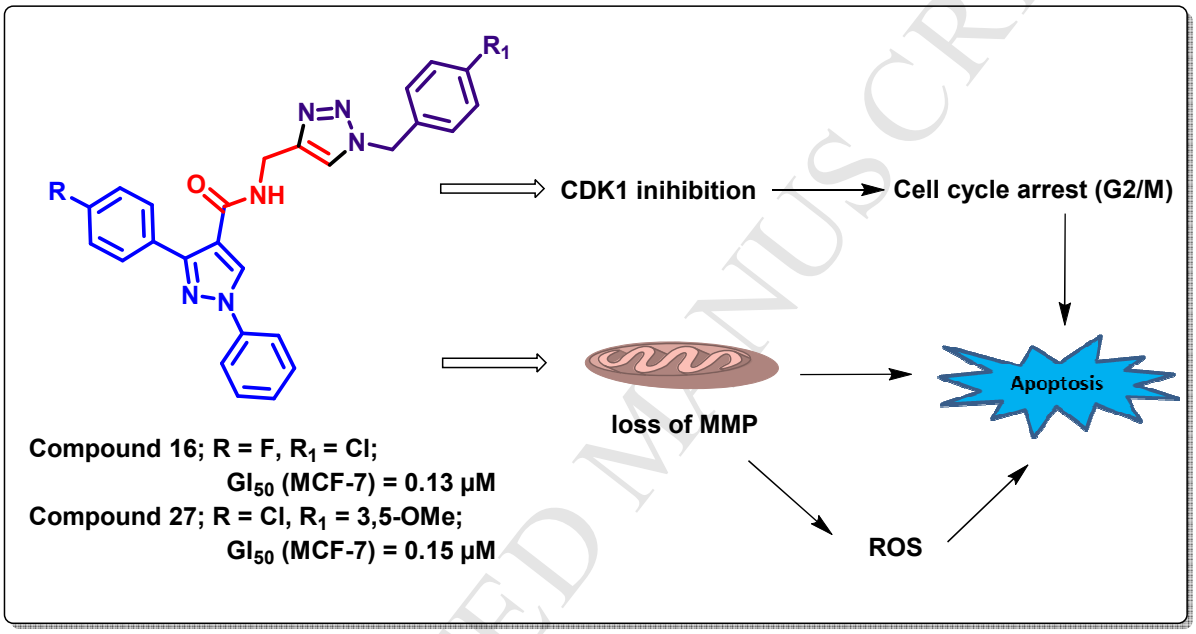

Design, synthesis and biological evaluation of *N*-((1-benzyl-1*H*-1,2,3-triazol-4-yl)methyl)-1,3-diphenyl-1*H*-pyrazole-4-carboxamides as CDK1/Cdc2 inhibitors

V. Ganga Reddy,[a] T. Srinivasa Reddy,[a,b] V. Lakshma Nayak,[a] Budaganaboyina Prasad,[a] Adiyala Praveen Reddy,[a] A. Ravikumar,[a,c] Shaik Taj,[a] Ahmed Kamal,[*a,b,c,d]

[a]*Medicinal Chemistry and Pharmacology, CSIR-Indian Institute of Chemical Technology, Hyderabad 500 007, India.*

[b]*IICT-RMIT Research Centre, CSIR-Indian Institute of Chemical Technology, Hyderabad 500 007, India.*

[c]*Department of Medicinal Chemistry, National Institute of Pharmaceutical Education and Research (NIPER), Hyderabad 500 037, India.*

[d]*Catalytic Chemistry Research Chair, Chemistry Department, College of Science, King Saud University, Riyadh 11451, Saudi Arabia.*

Abstract

A series of new (*N*-((1-benzyl-1*H*-1,2,3-triazol-4-yl)methyl)-1,3-diphenyl-1*H*-pyrazole-4-carboxamide derivatives (**8-35**) were designed, synthesized and evaluated as CDK1/Cdc2 inhibitors. Biological evaluation assays indicated that compounds **16** and **27** showed the most potent growth inhibitory activity against human cancer cell lines (MIAPaCa-2, MCF-7 and HeLa) with GI_{50} values ranging from 0.13 to 0.7 µM, compared with the positive control nocodazole (0.81-0.95 µM). Flow cytometric analysis revealed that these compounds induce cell cycle arrest in the G2/M phase and Western blot analysis suggested that compound treatment resulted in reduction of CDK1 expression levels in MCF-7 cell line. Moreover, the apoptosis inducing effect of the compounds was studied using Hoechst staining, Rhodamine 123 staining (MMP), carboxy-DCFDA staining (ROS), Annexin V-FITC assay. Based on these studies, two compounds **16** and **27** have been identified as promising new molecules that have the potential to be developed as leads.

Keywords:

Pyrazole; CDK1 inhibition; anti-cancer activity; cell cycle; apoptosis

1. Introduction

Cyclin-dependent kinases (CDKs) belong to a family of serine/threonine protein kinases which play a pivotal role in the regulation of the eukaryotic cell division, control of gene transcription and other processes of the cell cycle. The loss of cell cycle control provides an abnormal cell growth which is a major key characteristic point of cancer [1] and the inhibition of CDKs may provide an effective method for controlling tumor growth in cancer chemotherapy [2, 3], hence CDKs are known to play a key role in different types of human cancers [4]. In this progression, CDKs do not participate alone, it is associated with cyclin subunits and its inhibition is controlled by phosphorylation of the CDK subunits in different phases of cell cycle, such as G1, S and G2/M [5, 6]. Each cell cycle phase transitions are regulated by different cdk/cyclin complexes. From the known human CDKs, CDK1 (CDC2) is the most essential for the suitable execution of cell cycle [7] and cell division [8, 9]. The predominant binding partner for CDK1 is cyclin B, which activates CDK1 at the G2/M transition. Moreover, several small molecule inhibitors of anti-CDK drugs are in clinical development as a new generation anticancer chemotherapeutics [10, 11] and some of the selected CDK1 inhibitors are illustrated in Fig.1.

Heterocyclic moieties play an important role in synthetic organic chemistry due to their extensive applications in pharmaceutical, veterinary and agrochemical fields [12]. Among them pyrazole derivatives have gained considerable attention in the history of nitrogen heterocyclic chemistry due to their wide variety of biological activities such as anticancer, antimicrobial, antibacterial, antitubercular, antidepressant, antipyretic, antioxidant, analgesic and anti-inflammatory etc [13-18]. They have taken a leading position in the medicinal chemistry and are also being used as important pharmacophores in the field of drug design. In additon, triazole is a unique template that is associated with a number of biological activities and this moiety is an attractive option to use it as a structural component in the design of new molecules as it is stable in acidic/basic conditions [19], also has a high dipole moment and affords the possibility of forming hydrogen bonds with bimolecular targets [20].

Recently, our research group reported many pyrazole derivatives as potent anticancer and apoptosis inducing agents against human cancer cell lines [21-23]. In continuation to extend our research, herein we report the synthesis of a series of *N*-((1-benzyl-1*H*-1,2,3-triazol-4-yl)methyl)-1,3-diphenyl-1*H*-pyrazole-4-carboxamides and their biological evaluation. These

studies indicated that some compounds like **16** and **27** showed potent antiproliferative activity against some human cancer cell lines. The detailed biological and structure–activity relationship studies have also been carried out.

< **Fig. 1** >

2. Results and Discussion

2.1 Chemistry

The synthetic route for *N*-((1-benzyl-1*H*-1,2,3-triazol-4-yl)methyl)-1,3-diphenyl-1*H*-pyrazole-4-carboxamide analogs (**8–35)** is outlined in Scheme 1. The required precursors, 1,3-diphenyl pyrazolocarboxaldehydes (**4a-d)** were prepared by following the previously reported procedure [24]. These were oxidized to the corresponding 1,3-diphenyl-1*H*-pyrazole-4-carboxylic acids **(5a–d)** employing sodium chlorite-sulphamic acid. The carboxylic acids (**5a-d)** obtained were coupled with the propargylamine in the presence of *N*-(3-dimethylaminopropyl)-*N*¢-ethylcarbodiimide hydrochloride (EDCI), 4-(dimethylamino)pyridine (DMAP) and 1-hydroxybenzotriazole (HOBT) in dry DMF under nitrogen atmosphere to provide the corresponding terminal alkynes **(6a-d)**. By using click chemistry protocol, these terminal alkynes were allowed to react with the benzyl azides **(7a-g)** in the presence of $CuSO_4.5H_2O$ and sodium ascorbate in t-butyl alcohol and water (1:1) at room temperature to afford the triazole derivatives **(8-35)** in excellent yields (75-90%). To the best of our knowledge, these compounds are prepared for the first time and all compounds were characterized by spectroscopic studies (IR, ^{1}H NMR and MS).

< **Scheme 1** >

2.2 Antiproliferative activity

A sulforhodamine B assay was performed to evaluate the cytotoxic effects of these *N*-((1-benzyl-1*H*-1,2,3-triazol-4-yl)methyl)-1,3-diphenyl-1*H*-pyrazole-4-carboxamides (**8–35)** against three tumor cell lines: MIAPaCa-2 (pancreatic), MCF-7 (breast carcinoma) and HeLa (cervical) using nocodazole as the positive control and the growth inhibition values are listed in **Table 1**. These carboxamides (**8–35)** showed notable antiproliferative effects and most of the compounds from this series displayed potent broad-spectrum growth inhibitory activities against all the

tested cell lines. Most of the compounds showed significant growth inhibition (GI_{50}) values compared to the standard, wherein some of the compounds like **13, 16, 17, 18, 20, 22, 23, 25, 26, 27, 28, 29, 32, 33** and **34** showed promising GI_{50} values against multiple cancer cell lines and were comparable to the positive standard. From the Table 1, it is observed that they exhibit significant antiproliferative activity with GI_{50} values ranging from 0.13 to >100 µM and some of them showed enhanced activity compared to the positive control (ranging from 0.81 to 0.95 µM). Among them, **16, 17, 20** and **27** possess remarkable GI_{50} values, i.e., **16** showed promising cytotoxic activity with 0.28, 0.13 and 0.21 µM against MIAPaCa-2 (pancreatic), MCF-7 (breast carcinoma) and HeLa (cervical) cancer cell lines. Similarly **17** exhibited 0.76, 0.81 and 0.25 µM, whereas **20** showed 0.19, 2.5 and 0.36 µM and **27** showed 0.34, 0.15 and 0.73 µM values against these human cancer cell lines (MIAPaCa-2, MCF-7 and HeLa), respectively.

< **Table 1** >

Based on the antiproliferative activity data, the structure activity relationship (SAR) was examined for these carboxamides (**8–35)**. In this study, the pyarazole moiety has two aryl ring systems i.e ring A and B, all the compounds having electron donating methoxy as well as electron withdrawing groups like chloro, fluoro and trifluoro methyl groups on the ring systems (A and B) have been investigated. It is demonstrated that compounds **16, 17, 18, 20, 22, 23, 25, 26, 27** and **28**, with mono-substituted halogens (fluorine and chlorine) on the A ring, exhibited more potent activities than compounds with methoxy substitutions, respectively. In case of constant A ring substituents, and with a change of substituents on B ring the activities were examined. Among these, electron withdrawing chloro and trifluoromethyl substituents on the B-ring resulted in moderate to high cytotoxic activity (**16** and **17**) and whereas 3,5-disubstituted compound **27** having an electron-donating group showed notable values. The interesting biological activity exhibited by **16** and **27** prompted us to investigate their effects at the cellular level and to understand the mechanism responsible for cell death.

2.3 Cell cycle analysis

Many anticancer compounds exert their growth inhibitory effect either by arresting the cell or by induction of apoptosis or a combined effect of both cycle arrest and apoptosis [25, 26]. Moreover, regulation of the cell cycle and apoptosis are considered to be effective approaches in

the development of cancer therapeutics [27]. The screening results revealed that compounds **16** and **27** showed significant cytotoxic activity against human breast cancer cell line, MCF-7. Therefore, it was considered of interest to understand whether this inhibition of cell growth was on account of cell cycle arrest. In this study MCF-7 cells were treated with these compounds at 50 and 100 nM concentrations for 48 h. nocodazole was used as a reference compound in this study. The results shown in figure 2 indicated significant increase of DNA content in G2/M phase and subsequent reduction in G0/G1 phase in comparison to the control cells. Moreover, increasing the dose resulted in the increase in the amount of cells in G2/M phase, this indicates that they induce G2/M phase cell cycle arrest in a dose dependent manner.

< **Fig. 2** >

2.4 Effect of 16 and 27 on CDK1/Cdc2

The cyclin-dependent kinase (CDK) proteins play a key role in the cell-cycle regulation in eukaryotic cells [28]. Orderly cell-cycle progression requires CDK activation, which is mainly controlled by the expression of their activator subunit, cyclin. The complexation of CDK1 (Cdc2) with cyclin B is an important aspect in G2/M phase progression [29, 30]. In this context, MCF-7 cells were treated with **16** and **27** at different concentrations (50 and 100 nM) for 48 h and Western blot analysis was performed. Results indicated that there was a significant reduction of CDK1 (Cdc2) expression level particularly by **27** as shown in Fig.3.

< **Fig. 3** >

2.5 Molecular docking study

The promising cytotoxic activity shown by these pyrazolo-4-carboxamides prompted us to perform molecular docking studies with a view to understand the binding poses on cyclin-dependent kinase 1 (CDK-1) enzyme. The studies were performed at the LZ9 binding site of the CDK-1 (PDB ID: 4Y72) [31]. Docking studies revealed that these molecules fit well in the LZ9 binding site of the CDK-1 (Figure 4a).

< **Fig. 4** >

These compounds (**16** and **27)** exhibit hydrogen bonding with Leu83 residue of the target protein (red dashed line in Figs **4b**, **4c** and **4d**). The amide proton from these compounds show hydrogen bonding at the carbonyl group of Leu83. Moreover, the nitrogen present at the third position of the triazole ring shows additional hydrogen bonding with amide proton of the same amino acid residue in both the cases.

Besides this, these compounds (**16** and **27**) show hydrophobic interactions with the target protein. The 4-chloro and 3,5-dimethoxy benzyl ring of **16** and **27** respectively**,** show interactions with Thy15, Val18, Lys33, Val64, Phe80, Ala145 and Asp146. In addition, **27** also interacts with Asn133 and leu134 due to the presence of methoxy groups. The phenyl ring of **16** and **27** shows interactions with Gly11, Glu12 and Gln132, apart from the interaction with Asn133 by compound **16**. The 4-F and 4-Cl phenyl ring of **16** and **27** respectively interacts with Ile10, Phe82, Ser84, Met85 and Lys89 whereas **16** interacts with Lys20. Pyrazole moiety interactions with Asp86 and Leu135 and whereas the triazole ring interacts with Ala31, Glu81 and Leu83 in both the cases.

2.6 Apoptotic studies

Apoptosis is an orderly cellular process that takes place in physiological and pathological conditions, and plays an important role in tissue homeostasis. Disruption or inappropriate regulation of different apoptotic pathways result in the overgrowth of malignant cells [32, 33]. Thus, it is necessary to consider inducing cellular apoptosis as an effective approach in cancer treatment. Moreover, previous reports suggested that G2/M cell cycle arrest leads to apoptosis, thus the apoptotic inducing effect of these compounds on MCF-7 cell line has been studied.

2.6.1 Hoechst 33242 staining

To investigate the morphological changes induced by these compounds in MCF-7 cells, Hoechst staining has been carried out. Hoechst 33242 is a cell membrane permeable dye, which stains the live cells nuclei as uniformly light blue and apoptotic cells nuclei as bright blue nuclei on account of karyopyknosis and chromatin condensation [34]. MCF-7 cells were treated with various concentrations (50 and 100 nM) of these compounds (**16** and **27**) for 48 h and stained with Hoechst 33242. The results from Fig. 5 shows that control cells had no obvious morphological changes with most cell nuclei appeared as uniformly light blue nuclei. On the

contrary, the cells treated with 50 nM of **16** and **27** exhibited bright blue fluorescence because of chromatin condensation which is a typical characteristic of apoptosis. These apoptotic nuclei significantly increase with increasing the concentration of the compounds to 100 nM and this observation demonstrates that they induce apoptosis.

< **Fig. 5** >

2.6.2 Measurement of mitochondrial membrane potential (MMP)

Previous reports suggest that mitochondria plays an important role in the propagation of apoptosis and its dysfunction within the apoptotic process, and is often associated with loss of the mitochondrial inner transmembrane potential [35]. To investigate this possibility, MCF-7 cells were exposed to various concentrations (50 and 100 nM) of **16** and **27** for 48 h and were analyzed for rhodamine-123 uptake using fluorescence microscope. Uptake of rhodamine-123 into the mitochondria is driven by mitochondrial transmembrane potential. Mitochondria with normal cells retain the dye and gives strong green fluorescence, whereas apoptotic cells with depolarized mitochondria cannot retain the dye, which results in reduced green fluorescence. The results from the figure indicated that, more than 90% of the untreated control cells were functionally active with high rhodamine-123 green fluorescence (Fig.6). Cells treated with **16** and **27** resulted in reduction of green fluorescence intensity which is significant with further increase in the concentration of the compounds to 100 nM. Thus, decrease in DΨm by the **16** and **27** indicated that the mitochondrial apoptotic death-signal pathway plays a critical role in induction of apoptosis in MCF-7 cells.

< **Fig. 6** >

2.6.3 Measurement of reactive oxygen species (ROS)

Apoptosis can be induced by oxidative stress which may be mediated by the generation of reactive oxygen species (ROS). As these compounds are cytotoxic and induce apoptosis in MCF-7 cells. We then examined the effect of these compounds (**16** and **27**) on ROS generation using non-fluorescent carboxy-2,7-dichlorofluorescein diacetate (carboxy-DCFDA) dye which gets oxidized to the fluorescent dichlorofluorescein (DCF) by a variety of peroxides [36]. In this assay, MCF-7 cells were treated with different concentrations of both **16** and **27** for 48 h and

analyzed for DCF fluorescence. As seen from the Figure, there as not much DCF fluorescence (ROS positive cells) observed in the untreated MCF-7 cells, and this status remained unchanged when cells were incubated with the 50 nM concentrations of **16** and **27**. Whereas, there was a significant increase of DCF green fluorescence with 100 nM of by these compounds as compared to the control. Therefore these results demonstrate that compounds are potent inducers of ROS.

< **Fig. 7** >

2.6.4 Annexin V-FITC for apoptosis

The apoptotic effect of these compounds (**16** and **27**) was further evaluated by Annexin V FITC/PI (AV/PI) dual staining assay [37] to examine the occurrence of phosphatidylserine externalization and facilitates the detection of live cells (Q1-LL; AV-/PI-), early apoptotic cells (Q1-LR; AVþ/PI-), late apoptotic cells (Q1-UR-AVþ/ PIþ) and necrotic cells (Q1-UL; AV-/PIþ). In this study, MCF-7 cells were treated with these compounds for 48 h at 50 and 100 nM concentrations to examine the apoptotic effect. As shown in the figure 8, the percentage of total apoptotic cells significantly increased after treatment by these compounds. These results confirm a dose dependent apoptotic inducing effect by these compounds.

< **Fig. 8** >

3. Conclusion

In summary, we have designed and synthesized a series of *N*-((1-benzyl-1*H*-1,2,3-triazol-4-yl)methyl)-1,3-diphenyl-1*H*-pyrazole-4-carboxamides (**8-35**) and examined their cytotoxicity on three human cancer cell lines (MIAPaCa-2, MCF-7 and HeLa). The antiproliferative activity screening results indicated that most of these compounds exhibit potent growth inhibitory activity (GI_{50} values ranging from 0.13 to >100 µM). Interestingly, compounds **16** and **27** showed potent cytotoxic efficacy against the MCF-7 human cancer cell line. Treatment of MCF-7 cells with these compounds resulted in G2/M cell cycle arrest and down regulation of CDK1 expression in MCF-7 cells. Moreover, they induce apoptosis through depolarization of mitochondrial membrane potential and increased ROS production. Therefore, compounds they can be considered as interesting lead molecules for further development of more potent anticancer agents against breast cancer cells.

4. Experimental Section

All the starting materials and other reagents of the best grade were commercially available and were used without further purification. TLC was performed on 0.25 mm silica gel 60-F_{254} plates. Spots were visualized by UV light. All melting points were taken and are uncorrected. ^{1}H and ^{13}C NMR spectra were recorded on 75, 300 and 500 MHz spectrometers using tetramethylsilane as the internal standard. Chemical shifts are reported in parts per million (ppm) downfield from tetramethylsilane. Spin multiplicities are described as s (singlet), brs (broad singlet), d (doublet), dd (double doublet), t (triplet), q (quartet), or m (multiplet). Coupling constants are reported in hertz (Hz). HRMS analyses were acquired on single quadruple and carried out using the ESI techniques at 70 eV. Wherever required column chromatography was performed using silica gel of 60–120 mm with hexane and ethyl acetate as eluents.

4.1 General Procedure for the synthesis of 1,3-diphenyl-1*H*-pyrazole-4-carboxylic acids (5a-d)

The 1,3-diphenyl-1*H*-pyrazole-4-carboxylic acids (**4a-d**) were synthesized based on a literature method as following: para-substituted acetophenones (**1a-d,** 20 mmol) interact with phenyl hydrazine (**2**, 25 mmol) in anhydrous ethanol to form 1-phenyl-2-(1-phenylethylidene) hydrazine, which was added to a cold solution of DMF (25 mL) and $POCl_3$ (5 mL), stirred at 50–60 °C for 5 h. The resulting mixture was poured into ice-cold water, a saturated solution of sodium bi carbonate was added to neutralize the mixture, the obtained solid (1, 3-diphenyl-1*H*-pyrazole-4-carbaldehyde) precipitate was filtered, then after reaction with $NaClO_2$ and sulphamic acid in acetone to gave carboxylic acid derivatives **(5a-d)**.

4.2 General Procedure for the synthesis of Alkynes (6a-d)

To a solution of 1, 3-diphenyl-1*H*-pyrazole-4-carboxylic acid (2 mmol) in 10 mL of dry DMF, EDCI (2.4 mmol) and HOBT (2.4 mmol) were added at 0 °C and the reaction mixture was stirred for 20 min. To the reaction mixture propargylamine (2 mmol) was added and stirred overnight at room temperature for 12 h. The contents of the reaction mixture were poured into ice-cold water (50 mL), extracted with ethyl acetate. The organic layer was washed with saturated $NaHCO_3$ and

1N HCl, dried over Na_2SO_4 and concentrated *in vacuo*. The crude product was purified by column chromatography by using EtOAc/hexane as eluant.

4.2.1 1,3-diphenyl-*N*-(prop-2-ynyl)-1*H*-pyrazole-4-carboxamide (6a).

White solid, yield 74%, Mp: 131-133 °C; ^{1}H NMR (500 MHz, $CDCl_3$): δ 2.18 (t, *J* = 2.5 Hz, 1H), 4.10 (dd, *J* = 2.4, 5.3 Hz, 2H), 5.89 (s, 1H), 7.35 (t, *J* = 7.3 Hz, 1H), 7.46-7.53 (m, 5H), 7.71 (dd, *J* = 1.5, 8.0 Hz, 2H), 7.75 (d, *J* = 7.4 Hz, 2H), 8.51 (s, 1H). ^{13}C NMR (75 MHz, $CDCl_3$): δ 29.0, 71.5, 79.0, 117.3, 119.3, 127.3, 128.9, 129.1, 129.3, 129.5, 131.1, 131.9, 139.2, 150.9, 162.2. MS (ESI): *m/z* 302 $[M+H]^+$.

4.2.2 3-(4-fluorophenyl)-1-phenyl-*N*-(prop-2-ynyl)-1*H*-pyrazole-4-carboxamide (6b).

White solid, yield 78%, Mp: 165-167 °C; ^{1}H NMR (500 MHz, $CDCl_3$): δ 2.21 (t, *J* = 2.5 Hz, 1H), 4.13 (dd, *J* = 2.4, 5.3 Hz, 2H), 5.81 (s, 1H), 7.20 (t, *J* = 8.6 Hz, 2H), 7.36 (t, *J* = 7.4 Hz, 1H), 7.49 (t, *J* = 7.6 Hz, 2H), 7.76-7.71 (m, 4H), 8.47 (s, 1H). ^{13}C NMR (75 MHz, $CDCl_3$+DMSO): δ 28.1, 71.1, 80.0, 114.2 (d, J_{CF} = 21.4 Hz), 116.0, 118.3, 126.5, 128.2, 129.0, 129.5, 130.3 (d, J_{CF} = 7.6 Hz), 138.6, 150.6, 162.1 (d, J_{CF} = 246.9 Hz), 162.1. MS (ESI): *m/z* 320 $[M+H]^+$. HRMS (ESI) calcd for $C_{19}H_{15}ON_3F$ $[M+H]^+$ 320.11937; found: 320.11903.

4.2.3 3-(4-chlorophenyl)-1-phenyl-*N*-(prop-2-ynyl)-1*H*-pyrazole-4-carboxamide (6c).

White solid, yield 80%, Mp: 151-153 °C; ^{1}H NMR (500 MHz, $CDCl_3$): δ 2.23 (t, *J* = 2.4 Hz, 1H), 4.14 (dd, *J* = 2.4, 5.3 Hz, 2H), 5.82 (s, 1H), 7.36 (t, *J* = 7.3 Hz, 1H), 7.69 (m, 1H), 7.71 (m, 1H), 7.72-7.75 (m, 2H), 8.46 (s, 1H). ^{13}C NMR (75 MHz, $CDCl_3$+DMSO): δ 28.0, 71.7, 80.2, 116.3, 118.3, 126.6, 127.4, 129.1, 129.8, 129.9, 130.7, 133.0, 138.6, 150.1, 161.9. MS (ESI): *m/z* 336 $[M+H]^+$. HRMS (ESI) calcd for $C_{19}H_{15}ON_3Cl$ $[M+H]^+$ 336.08982; found: 336.08940.

4.2.4 3-(4-methoxyphenyl)-1-phenyl-*N*-(prop-2-ynyl)-1*H*-pyrazole-4-carboxamide (6d).

White solid, yield 75%, Mp: 176-178 °C; ^{1}H NMR (300 MHz, $CDCl_3$+DMSO): δ 2.53 (s, 1H), 2.98 (t, *J* = 2.2 Hz, 1H), 4.05 (dd, *J* = 2.2, 5.2 Hz, 2H), 6.96 (d, *J* = 8.6 Hz, 2H), 7.35 (t, *J* = 7.3 Hz, 1H), 7.53 (t, *J* = 7.9 Hz, 2H), 7.79-7.89 (m, 4H), 8.55 (t, *J* = 5.2 Hz, 1H), 8.86 (s, 1H). ^{13}C NMR (75 MHz, $CDCl_3$+DMSO): δ 28.0, 54.8, 72.4, 80.6, 113.0, 116.3, 118.3, 124.5, 126.5,

129.3, 129.6, 129.7, 138.9, 150.8, 159.2, 162.3. MS (ESI): *m/z* 332 $[M+H]^+$. HRMS (ESI) calcd for $C_{20}H_{18}O_2N_3$ $[M+H]^+$ 332.13935; found: 332.13852.

4.3 General Procedure for the synthesis of Click (8-35)

To a solution of alkynes (**6a-d**, 2 mmol) and corresponding aryl azides (**7a-g**, 2 mmol) in a mixture of t-BuOH/H_2O 1 : 1 (10 mL) was added $CuSO_4 \cdot 5H_2O$ (2 mmol) and sodium ascorbate (10 mmol). The reaction mixture was stirred at room temperature overnight. After completion of the reaction, the mixture was diluted with 50 ml of water and extracted with ethylacetate (2 X 25 ml), the combined organic phase was washed with brine, dried over anhydrous sodium sulfate, filtered and evaporated *in vacuo*. The crude product was purified by column chromatography by using EtOAc/hexane as eluant.

4.3.1 *N*-((1-(4-fluorobenzyl)-1*H*-1,2,3-triazol-4-yl)methyl)-1,3-diphenyl-1*H*-pyrazole-4-carboxamide (8).

Light brown solid, yield 79%, Mp: 134-136 °C; ^{1}H NMR (500 MHz, $CDCl_3$): δ 4.54 (d, *J* = 5.9 Hz, 2H), 5.45 (s, 2H), 6.33 (t, *J* = 5.4 Hz, 1H), 7.04-7.08 (m, 2H), 7.23-7.26 (m, 1H), 7.32-7.36 (m, 1H), 7.40 (d, *J* = 1.6 Hz, 1H), 7.41 (d, *J* = 1.9 Hz, 2H), 7.45-7.49 (m, 3H), 7.61-7.64 (m, 2H), 7.72-7.75 (m, 2H), 8.47 (s, 1H).^{13}C NMR (75 MHz, $CDCl_3$): δ 34.8, 53.3, 116.0 (d, J_{CF} = 21.4 Hz), 117.4, 119.2, 122.2, 127.2, 128.7, 129.0, 129.1, 129.4, 129.9 (d, J_{CF} = 8.2 Hz), 130.3 (d, J_{CF} = 1.6 Hz), 130.7, 131.8, 139.1, 151.1, 162.7 (d, J_{CF} = 248.0 Hz), 162.8. MS (ESI): *m/z* 453 $[M+H]^+$. HRMS (ESI) calcd for $C_{26}H_{21}ON_6F$ $[M+H]^+$ 453.18336; found: 453.18322.

4.3.2 *N*-((1-(4-chlorobenzyl)-1*H*-1,2,3-triazol-4-yl)methyl)-1,3-diphenyl-1*H*-pyrazole-4-carboxamide (9).

Light brown solid, yield 76%, Mp: 158-160 °C; ^{1}H NMR (500 MHz, $CDCl_3$): δ 4.53 (d, *J* = 5.7 Hz, 2H), 5.42 (s, 2H), 6.54 (t, *J* = 5.3 Hz, 1H), 7.17 (d, *J* = 8.3 Hz, 2H), 7.32 (d, *J* = 2.1 Hz, 2H), 7.33 (s, 1H), 7.38 (d, *J* = 1.3 Hz, 1H), 7.39 (d, *J* = 2.1 Hz, 2H), 7.45 (t, *J* = 8.3 Hz, 2H), 7.49 (s, 1H), 7.62-7.66 (q, *J* = 2.1, 4.2 Hz, 2H), 7.70 (d, *J* = 8.3 Hz, 2H), 8.46 (s, 1H). ^{13}C NMR (75 MHz, $CDCl_3$): δ 34.8, 53.3, 111.8, 117.4, 119.2, 122.4, 127.2, 128.7, 129.0, 129.1, 129.2, 129.3,

129.4, 130.7, 131.8, 132.9, 134.7, 139.1, 151.0, 162.8. MS (ESI): *m/z* 469 $[M+H]^+$. HRMS (ESI) calcd for $C_{26}H_{21}ON_6Cl$ $[M+H]^+$ 469.1544; found: 469.15341.

4.3.3 1,3-diphenyl-*N*-((1-(4-(trifluoromethyl)benzyl)-1*H*-1,2,3-triazol-4-yl)methyl)-1*H*-pyrazole-4-carboxamide (10).

Light brown solid , yield 81%, Mp: 152-154 °C; ^{1}H NMR (500 MHz, $CDCl_3$): δ 4.54 (d, *J* = 5.9 Hz, 2H), 5.52 (s, 2H), 6.53 (t, *J* = 5.4, 5.6 Hz, 1H), 7.30-7.35 (m, 3H), 7.39 (t, *J* = 3.3, 3.0 Hz, 3H), 7.45 (t, *J* = 8.2, 7.6 Hz, 2H), 7.52 (s, 1H), 7.61 (s, 1H), 7.62-7.65 (m, 3H), 7.72 (d, *J* = 7.9 Hz, 2H), 8.47 (s, 1H). ^{13}C NMR (75 MHz, $CDCl_3$): δ 34.9, 53.4, 117.4, 119.2, 122.5, 126.0 (q, J_{CF3} = 3.8 Hz), 127.3, 128.1, 128.8, 129.0, 129.1, 129.5, 130.7, 131.8, 138.4, 139.1, 145.3, 151.0, 162.8. MS (ESI): *m/z* 503 $[M+H]^+$. HRMS (ESI) calcd for C_{27} $H_{21}ON_6F_3$ $[M+H]^+$ 503.18017; found: 503.17995.

4.3.4 *N*-((1-(4-methoxybenzyl)-1*H*-1,2,3-triazol-4-yl)methyl)-1,3-diphenyl-1*H*-pyrazole-4-carboxamide (11).

White solid, yield 78%, Mp: 166-168 °C; ^{1}H NMR (300 MHz, $CDCl_3$): δ 3.80 (s, 3H), 4.53 (d, *J* = 5.8 Hz, 2H), 5.41 (s, 2H), 6.32 (t, *J* = 4.9, 4.7 Hz, 1H), 6.89 (d, *J* = 8.6 Hz, 2H), 7.22 (d, *J* = 8.4 Hz, 2H), 7.32 (d, *J* = 7.5 Hz, 1H), 7.35-7.42 (m, 4H), 7.47 (t, *J* = 8.1, 7.5 Hz, 2H), 7.62 (dd, *J* = 3.9, 1.8 Hz, 2H), 7.73 (d, *J* = 7.7 Hz, 2H), 8.47 (s, 1H). ^{13}C NMR (75 MHz, $CDCl_3$): δ 34.9, 53.6, 55.2, 114.4, 117.5, 119.3, 121.9, 126.4, 127.2, 128.7, 129.0, 129.1, 129.4, 129.6, 130.7, 131.8, 139.2, 144.8, 151.0, 159.8, 162.7. MS (ESI): *m/z* 465 $[M+H]^+$. HRMS (ESI) calcd for $C_{27}H_{24}O_2N_6$ $[M+H]^+$ 465.20335; found: 465.20293.

4.3.5 *N*-((1-(3,4-dimethoxybenzyl)-1*H*-1,2,3-triazol-4-yl)methyl)-1,3-diphenyl-1*H*-pyrazole-4-carboxamide (12).

White solid, yield 84%, Mp: 140-142 °C; ^{1}H NMR (500 MHz, $CDCl_3$): δ 3.82 (s, 3H), 3.86 (s, 3H), 4.53 (d, *J* = 5.7 Hz, 2H), 5.40 (s, 2H), 6.46 (s, 1H), 6.78 (s, 1H), 6.84 (s, 2H), 7.32 (t, *J* = 7.3 Hz, 1H), 7.38 (s, 3H), 7.42-7.48 (m, 3H), 7.62 (dd, *J* = 3.8 Hz, 3H), 7.72 (d, *J* = 7.9 Hz, 2H), 8.46 (s, 1H). ^{13}C NMR (75 MHz, $CDCl_3$): δ 34.9, 54.4, 55.9, 111.1, 111.2, 117.4, 119.2, 120.8, 122.0, 126.7, 127.2, 128.7, 128.9, 129.1, 129.4, 130.6, 131.8, 139.1, 144.8, 149.3, 149.4, 151.0,

162.7. MS (ESI): *m/z*495 $[M+H]^+$. HRMS (ESI) calcd for $C_{28}H_{26}O_3N_6$ $[M+H]^+$ 495.21392; found: 495.21333.

4.3.6 *N*-((1-(3,5-dimethoxybenzyl)-1*H*-1,2,3-triazol-4-yl)methyl)-1,3-diphenyl-1*H*-pyrazole-4-carboxamide (13).

Light brown solid, yield 76%, Mp: 171-173 °C; ^{1}H NMR (500 MHz, $CDCl_3$): δ 3.76 (s, 6H), 4.55 (d, *J* = 5.8 Hz, 2H), 5.40 (s, 2H), 6.30 (t, *J* = 5.4 Hz, 1H), 6.39 (bs, 2H), 6.43 (t, *J* = 2.2, 1.8 Hz, 1H),7.34 (t, *J* = 7.3 Hz, 1H), 7.38-7.42 (m, 3H), 7.43-7.52 (m, 3H), 7.74 (d, *J* = 7.5 Hz, 2H), 8.48 (s, 1H). ^{13}C NMR (75 MHz, $CDCl_3$): δ 34.9, 54.1, 55.3, 100.2, 106.1, 117.5, 119.2, 122.2, 127.2, 128.7, 129.0, 129.1, 129.4, 130.7, 131.8, 136.5, 139.2, 144.9, 151.1, 161.2, 162.7. MS (ESI): *m/z* 495 $[M+H]^+$. HRMS (ESI) calcd for $C_{28}H_{26}O_3N_6$ $[M+H]^+$ 495.21392; found: 495.21236.

4.3.7 1,3-diphenyl-*N*-((1-(3,4,5-trimethoxybenzyl)-1*H*-1,2,3-triazol-4-yl)methyl)-1*H*-pyrazole-4-carboxamide (14).

Light brown solid, yield 86%, Mp: 153-155 °C; ^{1}H NMR (500 MHz, $CDCl_3$): δ 3.80 (s, 6H), 3.82 (s, 3H), 4.55 (d, *J* = 5.7 Hz, 2H), 5.39 (s, 2H), 6.48 (s, 2H), 7.33 (t, *J* = 7.4 Hz, 1H), 7.37-7.41 (m, 3H), 7.45 (t, *J* = 8.2, 7.6 Hz, 2H), 7.52 (s, 1H), 7.63 (d, *J* = 4.2 Hz, 1H), 7.65 (d, *J* = 2.1 Hz, 1H), 7.73 (d, *J* = 7.6 Hz, 2H), 8.47 (s, 1H). ^{13}C NMR (75 MHz, $CDCl_3$): δ 34.9, 54.4, 56.1, 60.7, 105.2, 117.4, 119.2, 122.2, 127.2, 128.7, 128.9, 129.1, 129.4, 129.8, 130.7, 131.8, 139.1, 145.0, 151.0, 153.6, 162.7. MS (ESI): *m/z*524 $[M+H]^+$. HRMS (ESI) calcd for $C_{29}H_{28}O_4N_6$ $[M+H]^+$ 525.22448; found: 525.22404.

4.3.8 *N*-((1-(4-fluorobenzyl)-1*H*-1,2,3-triazol-4-yl)methyl)-3-(4-fluorophenyl)-1-phenyl-1*H*-pyrazole-4-carboxamide (15).

White solid, yield 80%, Mp: 164–166 °C; ^{1}H NMR (500 MHz, $CDCl_3$): δ 4.56 (s, 2H), 5.46 (s, 2H), 6.46 (s, 1H), 7.02-7.12 (m, 4H), 7.22-7.28 (m, 3H), 7.34 (t, *J* =7.3 Hz, 1H), 7.46 (t, *J* = 7.6, 7.9 Hz, 3H), 7.66 (t, *J* = 8.2 Hz, 3H), 7.72 (d, *J* = 7.9 Hz, 2H), 8.44 (s, 1H). ^{13}C NMR (75 MHz, $CDCl_3$): δ 34.9, 53.6, 115.6 (d, J_{CF} = 21.274 Hz), 116.1 (d, J_{CF} = 22.0 Hz), 117.2, 119.2, 127.3, 128.0 (d, J_{CF} = 2.9 Hz), 129.5, 129.9 (d, J_{CF} = 8.0 Hz), 130.1 (d, J_{CF} = 2.9 Hz), 130.4, 130.9 (d,

J_{CF} = 8.0 Hz), 139.1, 150.4, 162.8, 162.8 (d, J_{CF} = 248.6 Hz), 163.2 (d, J_{CF} = 248.6 Hz). MS (ESI): *m/z* 471 $[M+H]^+$. HRMS (ESI) calcd for $C_{26}H_{20}ON_6F_2$ $[M+H]^+$ 471.17394; found: 471.17356.

4.3.9 *N*-((1-(4-chlorobenzyl)-1*H*-1,2,3-triazol-4-yl)methyl)-3-(4-fluorophenyl)-1-phenyl-1*H*-pyrazole-4-carboxamide (16).

White solid, yield 82%, Mp: 174-176 °C; ^{1}H NMR (500 MHz, $CDCl_3$): δ 4.56 (s, 2H), 5.46 (s, 2H), 6.56 (s, 1H), 7.10 (t, *J* = 8.5 Hz, 2H), 7.19 (d, *J* = 8.2 Hz, 2H), 7.34 (d, *J* = 8.0 Hz, 2H), 7.46 (t, *J* = 7.9, 7.6 Hz, 2H), 7.65-7.70 (m, 3H), 7.72 (d, *J* = 7.7 Hz, 2H), 8.45 (s, 1H). ^{13}C NMR (75 MHz, $CDCl_3$): δ 34.9, 54.1, 115.6, 115.7 (d, J_{CF} = 20.8 Hz), 117.2, 117.3, 119.3, 128.0 (d, J_{CF} = 2.7 Hz), 128.8, 129.3, 129.4, 129.5, 130.8, 130.9 (d, J_{CF} = 8.1 Hz), 132.6, 134.9, 139.1, 150.4, 162.8, 163.2 (d, J_{CF} = 248.8 Hz). MS (ESI): *m/z* 487 $[M+H]^+$. HRMS (ESI) calcd for $C_{26}H_{20}ON_6ClF$ $[M+H]^+$ 487.14439; found: 487.14295.

4.3.10 3-(4-fluorophenyl)-1-phenyl-*N*-((1-(4-(trifluoromethyl)benzyl)-1*H*-1,2,3-triazol-4-yl)methyl)-1*H*-pyrazole-4-carboxamide (17).

Off white solid**,** yield 77%, Mp: 195-197 °C; ^{1}H NMR (300 MHz, $CDCl_3$): δ 3.36 (s, 2H), 4.54 (d, *J* = 5.28, 2H), 5.68 (s, 2H), 7.10 (t, *J* = 8.6 Hz, 2H), 7.34 (t, *J* = 7.3, 7.1 Hz, 1H), 7.46-7.54 (m, 4H), 7.65 (d, *J* = 8.1 Hz, 2H), 7.83 (d, *J* = 7.9 Hz, 2H), 7.88-7.94 (m, 2H), 8.04 (s,1H), 8.62 (t, *J* = 5.0 Hz, 1H), 8.88 (s, 1H). ^{13}C NMR (75 MHz, $CDCl_3$): δ 34.8, 53.3, 55.2, 114.2, 117.1, 119.1, 122.6, 124.0, 126.0 (q, J_{CF3} = 3.2 Hz), 127.1, 128.1, 129.4, 130.3, 130.6, 134.0, 138.3, 139.1, 145.3, 150.9, 160.2, 162.9. MS (ESI): *m/z* 521 $[M+H]^+$. HRMS (ESI) calcd for $C_{27}H_{20}ON_6F_4$ $[M+H]^+$ 521.17075; found: 521.17106.

4.3.11 3-(4-fluorophenyl)-*N*-((1-(4-methoxybenzyl)-1*H*-1,2,3-triazol-4-yl)methyl)-1-phenyl-1*H*-pyrazole-4-carboxamide (18).

Off white solid, yield 84%, Mp: 184-186 °C; ^{1}H NMR (300 MHz, $CDCl_3$): δ 3.80 (s, 3H), 4.60 (s, 2H), 5.40 (s, 2H), 6.84 (d, *J* = 8.1 Hz, 2H), 7.06 (t, *J* = 8.1, 8.3 Hz, 2H), 7.20 (d, *J* = 8.3 Hz, 2H),7.33 (t, *J* = 7.3 Hz, 1H), 7.46 (t, *J* = 7.7, 7.3 Hz, 2H), 7.64-7.74 (m, 4H), 8.46 (s, 1H). ^{13}C NMR (75 MHz, $CDCl_3$): δ 34.79, 54.2, 55.2, 114.4, 115.5 (d, J_{CF} = 21.9 Hz), 117.2, 119.24,

126.1, 127.2, 128.0, 129.4, 129.6, 130.4, 130.5, 130.9 (d, J_{CF} = 8.2 Hz), 139.1, 150.5, 159.9, 162.7, 163.1 (d, J_{CF} = 248.6 Hz). MS (ESI): *m/z* 483 $[M+H]^+$. HRMS (ESI) calcd for $C_{27}H_{23}O_2N_6F$ $[M+H]^+$ 483.19393; found: 483.19386.

4.3.12 *N*-((1-(3,4-dimethoxybenzyl)-1*H*-1,2,3-triazol-4-yl)methyl)-3-(4-fluorophenyl)-1-phenyl-1*H*-pyrazole-4-carboxamide (19).

Off white solid, yield 76%, Mp: 175-177 °C; ^{1}H NMR (500 MHz, $CDCl_3$): δ 3.82 (s, 3H), 3.86 (s, 3H), 4.55 (d, *J* = 5.7 Hz, 2H), 5.40 (s, 2H), 6.78 (s, 2H), 6.82-6.85 (m, 2H), 7.06 (t, *J* = 8.6 Hz, 2H), 7.32 (t, *J* = 7.3, 7.4 Hz, 1H), 7.44 (t, *J* = 8.3, 7.4 Hz, 2H), 7.51 (s, 1H), 7.65-7.72 (m ,4H), 8.45 (s, 1H). ^{13}C NMR (75 MHz, $CDCl_3$): δ 34.8, 54.0, 55.8, 111.1 (d, J_{CF} = 6.5 Hz), 115.6 (d, J_{CF} = 21.9 Hz), 117.2, 119.2, 120.8, 122.1, 126.6, 127.2, 127.9, 129.4, 130.3, 130.9 (d, J_{CF} = 8.2 Hz), 139.1, 144.8, 149.3, 149.4, 150.4, 162.7, 163.1 (d, J_{CF} = 249.1 Hz); MS (ESI): *m/z* 513 $[M+H]^+$. HRMS (ESI) calcd for $C_{28}H_{25}O_3N_6F$ $[M+H]^+$ 513.20449; found: 513.20435.

4.3.13 *N*-((1-(3,5-dimethoxybenzyl)-1*H*-1,2,3-triazol-4-yl)methyl)-3-(4-fluorophenyl)-1-phenyl-1*H*-pyrazole-4-carboxamide (20).

Off white solid, yield 88%, Mp: 181-183 °C; ^{1}H NMR (300 MHz, $CDCl_3$): δ 3.74 (s, 6H), 4.56 (bs, 2H), 5.38 (s, 2H), 6.37 (s, 2H), 6.42 (s, 1H), 6.90 (s, 1H), 7.06 (t, *J* = 8.6, 8.4 Hz, 2H), 7.32 (d, *J* = 7.3 Hz, 1H), 7.43 (t, *J* = 7.9, 7.5 Hz, 2H), 7.64-7.74 (m ,4H), 8.47 (s, 1H). ^{13}C NMR (75 MHz, $CDCl_3$): δ 34.8, 54.2, 55.3, 100.2, 106.1, 115.5 (d, J_{CF} = 21.9 Hz), 117.1, 119.2, 127.2, 128.0 (d, J_{CF} = 2.7 Hz), 129.4, 130.2, 130.8 (d, J_{CF} = 8.2 Hz), 136.3, 139.1, 150.5, 161.2, 162.8, 163.1 (d, J_{CF} = 248.6 Hz); MS (ESI): *m/z* 513 $[M+H]^+$. HRMS (ESI) calcd for $C_{28}H_2O_3N_6F$ $[M+H]^+$ 513.20449; found: 513.20364.

4.3.14 3-(4-fluorophenyl)-1-phenyl-*N*-((1-(3,4,5-trimethoxybenzyl)-1*H*-1,2,3-triazol-4-yl)methyl)-1*H*-pyrazole-4-carboxamide (21).

Off white solid, yield 76%, Mp: 189-191 °C; ^{1}H NMR (500 MHz, $CDCl_3$): δ 3.80(s, 6H), 3.82 (s, 3H), 4.57 (d, *J* = 5.7 Hz, 2H), 5.39 (s, 2H), 6.49 (s, 2H), 6.72 (t, *J* = 5.6 Hz, 1H), 7.08 (t, *J* = 8.6, 8.8 Hz, 2H), 7.33 (t, *J* = 7.4, 7.3 Hz, 1H), 7.45 (t, *J* = 8.3, 7.6 Hz, 2H), 7.55 (s, 1H), 7.65-7.77 (m, 1H), 7.72 (dd, *J* = 7.6, 1.2 Hz, 2H), 8.45 (s, 1H). ^{13}C NMR (75 MHz, $CDCl_3$): δ 34.8, 54.4,

56.1, 60.7, 105.2, 115.6 (d, J_{CF} = 21.4 Hz), 117.1, 119.2, 122.3, 127.3, 127.9 (d, J_{CF} = 2.7 Hz), 129.4, 129.7, 130.2, 130.9 (d, J_{CF} = 8.7 Hz), 138.2, 139.1, 144.9, 150.4, 153.6, 162.8, 163.1 (d, J_{CF} = 248.6 Hz); MS (ESI): *m/z* 543 $[M+H]^+$. HRMS (ESI) calcd for $C_{29}H_{27}O_4N_6F$ $[M+H]^+$ 543.21506; found: 543.21488.

4.3.15 3-(4-chlorophenyl)-*N*-((1-(4-fluorobenzyl)-1*H*-1,2,3-triazol-4-yl)methyl)-1-phenyl-1*H*-pyrazole-4-carboxamide (22).

Off white solid, yield 82%, Mp: 183-185 °C; ^{1}H NMR (500 MHz, $CDCl_3$): δ 4.58 (s, 2H), 5.42 (s, 2H), 6.70 (s, 1H), 7.06 (t, *J* = 8.3 Hz, 2H), 7.20 (d, *J* = 4.7 Hz, 1H), 7.36 (t, *J* = 9.1, 8.2 Hz, 3H), 7.42 (t, *J* = 7.6 Hz, 2H), 7.65 (d, *J* = 8.8 Hz, 2H), 7.72 (d, *J* = 7.7 Hz, 2H), 8.44 (s, 1H). ^{13}C NMR (75 MHz, $CDCl_3$): δ 35.0, 53.8, 116.1 (d, J_{CF} = 21.9 Hz), 116.5, 117.2, 119.2, 127.3, 128.6, 129.4, 129.7, 130.0 (d, J_{CF} = 8.2 Hz), 130.2, 130.4, 131.5, 134.8, 139.0, 150.3, 162.8, 162.9 (d, J_{CF} = 248.6 Hz); MS (ESI): *m/z* 487 $[M+H]^+$. HRMS (ESI) calcd for $C_{26}H_{20}ON_6ClF$ $[M+H]^+$ 487.14439; found: 487.14549.

4.3.16 *N*-((1-(4-chlorobenzyl)-1*H*-1,2,3-triazol-4-yl)methyl)-3-(4-chlorophenyl)-1-phenyl-1*H*-pyrazole-4-carboxamide (23).

Off white solid, yield 80%, Mp: 168-170 °C; ^{1}H NMR (500 MHz, CDCl3): δ 4.57 (d, *J* = 5.7 Hz, 2H), 5.46 (s, 2H), 6.38-6.58 (m, 1H) 7.20(d, *J* = 8.3 Hz, 2H), 7.33-7.40 (m, 5H), 7.45-7.50 (m, 3H), 7.64 (d, *J* = 8.3 Hz, 2H), 7.72 (d, *J* = 8.2 Hz, 2H), 8.42 (s, 1H). ^{13}C NMR (75 MHz, $CDCl_3$): δ 34.8, 53.6, 115.7, 117.1, 119.2, 120.7, 127.3, 127.9, 128.0, 128.6, 129.2, 129.4, 130.4, 130.9, 132.7, 134.8, 139.0, 150.5, 163.8; MS (ESI): *m/z* 503 $[M+H]^+$. HRMS (ESI) calcd for $C_{26}H_{20}ON_6Cl_2$ $[M+H]^+$ 503.11484; found: 503.11666.

4.3.17 3-(4-chlorophenyl)-1-phenyl-*N*-((1-(4-(trifluoromethyl)benzyl)-1*H*-1,2,3-triazol-4-yl)methyl)-1*H*-pyrazole-4-carboxamide (24).

Off white solid, yield 82%, Mp: 173-175 °C; ^{1}H NMR (500 MHz, $CDCl_3$): δ 4.58 (d, *J* = 5.7 Hz, 2H), 5.55 (s, 2H), 6.52 (t, *J* = 5.6, 5.4 Hz, 1H), 7.26 (t, *J* = 8.5, 7.4 Hz, 2H), 7.32-7.36 (m, 2H), 7.37 (s, 2H), 7.39 (s, 1H), 7.54 (s, 1H), 7.64 (t, *J* = 8.3, 8.5 Hz, 4H), 7.72 (d, *J* = 7.4 Hz, 2H), 8.42 (s, 1H). ^{13}C NMR (75 MHz, $CDCl_3$): δ 34.8, 53.4, 117.1, 119.1, 122.7, 126.0 (q, J_{CF3} = 3.2

Hz), 127.3, 128.1, 128.6, 129.4, 130.2, 130.4, 130.7, 131.2, 134.8, 138.2, 139.0, 145.3, 150.3, 162.9; MS (ESI): *m/z* 537 $[M+H]^+$. HRMS (ESI) calcd for $C_{27}H_{20}ON_6ClF_3$ $[M+H]^+$ 537.14120; found: 537.14268.

4.3.18 3-(4-chlorophenyl)-*N*-((1-(4-methoxybenzyl)-1*H*-1,2,3-triazol-4-yl)methyl)-1-phenyl-1*H*-pyrazole-4-carboxamide (25).

Off white solid, yield 84%, Mp: 151-153 °C; ^{1}H NMR (500 MHz, $CDCl_3$): δ 3.80 (s, 3H), 4.55 (d, *J* = 5.7 Hz, 2H), 5.42 (s, 2H), 6.55 (m, 1H), 6.88 (d, *J* = 8.5 Hz, 2H), 7.33 (m, 3H), 7.44 (m, 3H), 7.62 (d, *J* = 8.5 Hz, 2H), 7.70 (d, *J* = 7.6 Hz, 2H), 8.46 (s, 1H). ^{13}C NMR (75 MHz, $CDCl_3$): δ 34.8, 53.7, 55.2, 114.4, 117.2, 119.2, 122.2, 126.2, 127.2, 128.6, 129.4, 129.6, 130.2, 130.4, 134.8, 139.1, 144.8, 150.2, 159.8, 162.8; MS (ESI): *m/z* 499 $[M+H]^+$. HRMS (ESI) calcd for $C_{27}H_{23}O_2N_6Cl$ $[M+H]^+$ 499.16438; found: 499.16414.

4.3.19 3-(4-chlorophenyl)-*N*-((1-(3,4-dimethoxybenzyl)-1*H*-1,2,3-triazol-4-yl)methyl)-1-phenyl-1*H*-pyrazole-4-carboxamide (26).

Off white solid, yield 77%, Mp: 155-157 °C; ^{1}H NMR (300 MHz, $CDCl_3$): δ 3.80 (s, 3H), 3.82 (s, 3H), 4.58 (s, 2H), 5.40 (s, 2H), 6.78 (s, 1H), 6.84 (s, 2H), 7.00 (s, 1H), 7.28- 7.38 (m, 3H), 7.44 (t, *J* = 7.3, 7.5 Hz, 2H), 7.68 (q, *J* = 7.7, 8.1 Hz, 5H), 8.46 (s, 1H). ^{13}C NMR (75 MHz, $CDCl_3$): δ 34.7, 54.1, 55.8, 111.0, 111.1, 117.1, 119.1, 120.8, 126.5, 127.2, 128.5, 129.4, 130.2, 130.4, 134.7, 139.0, 149.2, 149.3, 150.4, 162.8; MS (ESI): *m/z* 529 $[M+H]^+$. HRMS (ESI) calcd for $C_{28}H_{25}O_3N_6Cl$ $[M+H]^+$ 529.17494; found: 529.17610.

4.3.20 3-(4-chlorophenyl)-*N*-((1-(3,5-dimethoxybenzyl)-1*H*-1,2,3-triazol-4-yl)methyl)-1-phenyl-1*H*-pyrazole-4-carboxamide (27).

Off white solid, yield 84%, Mp: 186-188 °C; ^{1}H NMR (500 MHz, $CDCl_3$): δ 3.74 (s, 6H), 4.58 (s, 2H), 5.40 (s, 2H), 6.38 (s, 2H), 6.40 (s, 1H), 6.60 (s, 1H), 7.30-7.40 (m, 3H), 7.45 (t, *J* = 3.2, 7.6 Hz, 2H), 7.65 (d, *J* = 7.7 Hz, 2H), 7.72 (d, *J* = 7.6 Hz, 2H), 8.44 (s, 1H).^{13}C NMR (75 MHz, $CDCl_3$+DMSO): δ 33.1, 51.6, 53.5, 98.0, 104.4, 115.4, 117.0, 125.3, 126.1, 127.8, 128.5, 128.6, 129.6, 131.8, 136.0, 137.4, 148.8, 159.2, 160.9. MS (ESI): *m/z* 529 $[M+H]^+$. HRMS (ESI) calcd for $C_{28}H_{25}O_3N_6Cl$ $[M+H]^+$ 529.17494; found: 529.17604.

4.3.21 3-(4-chlorophenyl)-1-phenyl-*N*-((1-(3,4,5-trimethoxybenzyl)-1*H*-1,2,3-triazol-4-yl)methyl)-1*H*-pyrazole-4-carboxamide (28).

Off white solid**,** yield 89%, Mp: 149-151 °C; ^{1}H NMR (500 MHz, $CDCl_3$): δ 3.80 (s, 9H), 4.58 (d, *J* = 5.6 Hz, 2H), 5.40 (s, 2H), 6.50 (s, 2H), 6.56 (m, 1H), 7.32-7.40 (m, 3H), 7.46 (t, *J* = 7.1, 8.3 Hz, 2H), 7.54 (s, 1H), 7.66 (d, *J* = 8.3 Hz, 2H), 7.72 (d, *J*= 8.3 Hz, 2H), 8.43 (s, 1H). ^{13}C NMR (75 MHz, $CDCl_3$): δ 30.8, 34.8, 54.4, 56.0, 60.7, 105.2, 117.1, 119.2, 122.4, 127.3, 128.6, 129.4, 129.7, 130.1, 130.2, 130.3, 134.8, 139.0, 144.9, 150.3, 153.5, 162.8; MS (ESI): *m/z* 559 $[M+H]^+$. HRMS (ESI) calcd for $C_{29}H_{27}O_4N_6Cl$ $[M+H]^+$ 559.18551; found: 559.18421.

4.3.22 *N*-((1-(4-fluorobenzyl)-1*H*-1,2,3-triazol-4-yl)methyl)-3-(4-methoxyphenyl)-1-phenyl-1*H*-pyrazole-4-carboxamide (29).

White solid, yield 79%, Mp: 168-170 °C; ^{1}H NMR (500 MHz, $CDCl_3$): δ 3.85 (s, 3H), 4.53 (d, *J* = 5.7 Hz, 2H), 5.44 (s, 2H), 6.51 (t, *J* = 5.3 Hz, 1H), 6.93 (d, *J* = 7.3 Hz, 2H), 7.05 (t, *J* = 7.3, 8.3 Hz, 2H), 7.22-7.27 (m, 2H), 7.32 (t, *J* = 7.0, 7.7 Hz, 1H), 7.45 (t, *J* = 7.1 Hz, 2H), 7.50 (s, 1H), 7.56 (d, *J* = 8.5 Hz, 2H), 7.71 (d, *J* = 8.2 Hz, 2H), 8.45 (s, 1H).^{13}C NMR (75 MHz, $CDCl_3$): δ 34.8, 53.3, 55.3, 114.2, 116.0 (d, J_{CF} = 21.7 Hz), 117.2, 119.2, 122.2, 124.0, 127.1, 129.4, 129.9 (d, J_{CF} = 8.1 Hz), 130.3 (d, J_{CF} = 2.7 Hz), 130.6, 139.2, 145.1, 150.9, 160.2, 162.7 (d, J_{CF} = 247.9 Hz), 162.9 ; MS (ESI): *m/z* 483 $[M+H]^+$. HRMS (ESI) calcd for $C_{27}H_{23}O_2N_6F$ $[M+H]^+$ 483.19393; found: 483.19457.

4.3.23 *N*-((1-(4-chlorobenzyl)-1*H*-1,2,3-triazol-4-yl)methyl)-3-(4-methoxyphenyl)-1-phenyl-1*H*-pyrazole-4-carboxamide (30).

Off white solid, yield 82%, Mp: 160-162 °C; ^{1}H NMR (300 MHz, $CDCl_3$): δ 3.82 (s, 3H), 4.52 (d, *J* = 5.8 Hz, 2H), 5.42 (s, 2H), 6.62 (t, *J* = 5.6, 5.4 Hz, 1H), 6.92 (d, *J* = 8.6 Hz, 2H), 7.17 (d, *J* = 8.3 Hz, 2H), 7.32 (d, *J* = 8.1 Hz, 3H) 7.44 (t, *J* = 8.1, 7.5 Hz, 2H) 7.50 (s, 1H), 7.57 (d, *J* = 8.8 Hz, 2H), 7.70 (d, *J* = 7.9 Hz, 2H), 8.45 (s, 1H).^{13}C NMR (75 MHz, $CDCl_3$): δ 34.8, 53.3, 55.3, 114.2, 117.2, 119.2, 122.3, 124.0, 127.1, 129.2, 129.3, 129.4, 130.3, 130.5, 132.9, 134.75, 139.2, 145.2, 150.9, 160.2, 162.9; MS (ESI): *m/z* 499 $[M+H]^+$.HRMS (ESI) calcd for $C_{27}H_{23}O_2N_6Cl$ $[M+H]^+$499.16438; found: 499.16555.

4.3.24 3-(4-methoxyphenyl)-1-phenyl-*N*-((1-(4-(trifluoromethyl)benzyl)-1*H*-1,2,3-triazol-4-yl)methyl)-1*H*-pyrazole-4-carboxamide (31).

Off white solid, yield 80%, Mp: 145-147 °C; ^{1}H NMR (500 MHz, $CDCl_3$): δ 3.84 (s, 3H), 4.55 (d, *J* = 5.7 Hz, 2H), 5.53 (s, 2H), 6.55 (s, 1H), 6.94 (d, *J* = 8.6 Hz, 2H), 7.30-7.36 (m, 3H), 7.45 (t, *J* = 7.6, 8.2 Hz, 2H), 7.54 (s, 1H), 7.56 (s, 1H), 7.58 (s, 1H), 7.62 (d, *J* = 7.9 Hz, 2H), 7.72 (d, *J* = 8.3 Hz, 2H), 8.45 (s, 1H). ^{13}C NMR (75 MHz, $CDCl_3$): δ 34.8, 53.3, 55.2, 114.2, 117.1, 119.1, 122.6, 124.0, 126.0 (q, J_{CF3} = 3.2 Hz), 127.1, 128.1, 129.4, 130.3, 130.6, 138.3, 139.1, 145.3, 150.9, 160.2, 162.9; MS (ESI): *m/z* 533 $[M+H]^+$. HRMS (ESI) calcd for $C_{28}H_{23}O_2N_6F_3$ $[M+H]^+$ 533.19074; found: 533.19158.

4.3.25 *N*-((1-(4-methoxybenzyl)-1*H*-1,2,3-triazol-4-yl)methyl)-3-(4-methoxyphenyl)-1-phenyl-1*H*-pyrazole-4-carboxamide (32).

Off white solid, yield 78%, Mp: 170-172 °C; ^{1}H NMR (300 MHz, $CDCl_3$): δ 3.73 (s, 6H), 3.83 (s, 3H), 4.55 (bs, 2H), 5.38 (s, 2H), 6.35- 6.42 (m, 3H), 6.63 (s, 1H), 6.93 (d, *J* = 8.4 Hz, 2H), 7.30 (t, *J* = 7.3 Hz, 1H), 7.44 (t, *J* = 7.5, 7.9 Hz, 2H), 7.57 (d, *J* = 8.4 Hz, 3H), 7.70 (d, *J* = 7.7 Hz, 2H), 8.46 (s, 1H). ^{13}C NMR (75 MHz, $CDCl_3$): δ 34.8, 53.7, 55.2, 55.3, 114.2, 114.4, 117.3, 119.2, 122.0, 124.0, 126.4, 127.1, 129.4, 129.6, 130.3, 130.6, 139.2, 150.9, 159.8, 160.2, 162.8. MS (ESI): *m/z* 495 $[M+H]^+$. HRMS (ESI) calcd for $C_{28}H_{26}O_3N_6$ $[M+H]^+$ 495.21392; found: 495.21245.

4.3.26 *N*-((1-(3,4-dimethoxybenzyl)-1*H*-1,2,3-triazol-4-yl)methyl)-3-(4-methoxyphenyl)-1-phenyl-1*H*-pyrazole-4-carboxamide (33).

White solid, yield 75%, Mp: 143-145 °C; ^{1}H NMR (500 MHz, $CDCl_3$): δ 3.81 (s, 3H), 3.84 (s, 3H), 3.86 (s, 3H), 4.53 (d, *J* = 5.7 Hz, 2H), 5.40 (s, 2H), 6.55 (t, *J* = 5.3 Hz, 1H), 6.78 (s, 1H), 6.84 (s, 2H), 6.93 (d, *J* = 8.6 Hz, 2H), 7.32 (t, *J* = 7.4, 7.3 Hz, 1H), 7.45 (t, *J* = 8.0, 7.6 Hz, 2H), 7.49 (s, 1H), 7.57 (d, *J* = 8.6 Hz, 2H), 7.71 (d, *J* = 7.6 Hz, 2H), 8.45 (s, 1H). ^{13}C NMR (75 MHz, $CDCl_3$): δ 34.8, 54.0, 55.2, 55.8, 111.0, 111.1, 114.1, 117.1, 119.1, 120.7, 122.1, 124.0, 126.7, 127.1, 129.4, 130.3, 130.5, 139.1, 144.9, 149.3, 150.9, 160.2, 162.9; MS (ESI): *m/z* 525 $[M+H]^+$. HRMS (ESI) calcd for $C_{29}H_{28}O_4N_6$ $[M+H]^+$ 525.22448; found: 525.22504.

4.3.27 *N*-((1-(3,5-dimethoxybenzyl)-1*H*-1,2,3-triazol-4-yl)methyl)-3-(4-methoxyphenyl)-1-phenyl-1*H*-pyrazole-4-carboxamide (34).

White solid, yield 81%, Mp: 165-167 °C; ^{1}H NMR (500 MHz, $CDCl_3$): δ 3.75 (s, 6H), 3.86 (s, 3H), 4.55 (d, *J* = 5.0 Hz, 2H), 5.40 (S, 2H), 6.33-6.43 (m, 4H), 6.95 (d, *J* = 8.5 Hz, 2H), 7.33 (t, *J* = 7.3 Hz, 1H), 7.46 (t, *J* = 7.6 Hz, 2H), 7.49 (s, 1H), 7.56 (d, *J* = 8.6 Hz, 2H), 7.73 (d, *J* = 7.7 Hz, 2H), 8.45 (s, 1H). ^{13}C NMR (75 MHz, $CDCl_3$): δ 34.9, 54.2, 55.3, 100.3, 106.1, 114.3, 117.4, 119.3, 124.0, 127.2, 129.5, 130.4, 130.7, 136.5, 139.2, 150.9, 160.3, 161.2. MS (ESI): m/z 525 $[M+H]^+$. HRMS (ESI) calcd for $C_{29}H_{28}O_4N_6$ $[M+H]^+$ 525.22448; found: 525.22506.

4.3.28 3-(4-methoxyphenyl)-1-phenyl-*N*-((1-(3,4,5-trimethoxybenzyl)-1*H*-1,2,3-triazol-4-yl)methyl)-1*H*-pyrazole-4-carboxamide (35).

White solid, yield 76%, Mp: 153-155 °C; ^{1}H NMR (300 MHz, $CDCl_3$): δ 3.80 (s, 6H), 3.82 (s, 3H), 3.84 (s, 3H), 4.54 (d, *J* = 5.8 Hz, 2H), 5.38 (s, 2H), 6.48 (s, 2H), 6.60-6.66 (m, 1H), 6.93 (d, *J* = 7.5 Hz, 2H), 7.32 (d, *J* = 7.3 Hz, 1H), 7.44 (t, *J* = 6.9 Hz, 2H), 7.55 (d, *J* = 4.3 Hz, 2H), 7.58 (s, 1H), 7.72 (d, *J* = 8.4 Hz, 2H), 8.45 (s, 1H). ^{13}C NMR (75 MHz, $CDCl_3$): δ 34.8, 54.3, 55.2, 56.1, 60.7, 105.2, 114.2, 117.1, 119.1, 122.2, 124.0, 129.4, 129.8, 130.3, 130.5, 138.2, 139.1, 145.0, 150.9, 153.5, 160.2, 162.9; MS (ESI): *m/z* 555 $[M+H]^+$. HRMS (ESI) calcd for $C_{30}H_{30}O_5N_6$ $[M+H]^+$ 555.23504; found: 555.23647.

4.4 Biology

4.4.1 Cell culture

The cell lines, MIA PaCa-2 (pancreatic), MCF-7 (breast), HeLa (cervical) which were used in this study were procured from American Type Culture Collection (ATCC), United States and were maintained in the Dulbecco's modified Eagle's medium containing 10% (v/v) fetal bovine serum (FBS; HyClone, Logan, UT) supplemented with 100 units/mL of penicillin and streptomycin (Sigma-Aldrich, St. Louis, MO). All cells were cultured at 37 ºC in a humidified atmosphere with 5% CO_2. Test compounds were dissolved in DMSO (Sigma-Aldrich) to prepare 10 mM stock solution for the following experiments. The stock was diluted with culture medium to desired concentrations for drug treatment.

4.4.2 Evaluation of anti-proliferative activity

The anti-proliferative activity of the synthesized pyrazole derivatives was evaluated using SRB assay. A protocol of 48 h continuous drug exposure was used to estimate cell viability or growth. MiaPaca-2, MCF-7 and HeLa cells were seeded in 96-well plates in 100 µL aliquots at plating densities depending on the doubling time of individual cell lines. The microtiter plates were incubated at 37 °C, 5% CO_2, 95% air, and 100% relative humidity for 24 h and then cells were treated with different doses (0.01, 0.1, 1, 10, 100 µM) of synthesized compounds. After 48 hours incubation at 37 °C, cells were fixed with 10% (wt/vol) cold trichloroacetic acid and incubated at 4 °C for 1h and were then stained with 0.057% SRB dissolved in 1% acetic acid for 30 min at room temperature. Unbound SRB was washed with 1% acetic acid. The protein–bound dye was dissolved in 10mM Tris base solution for OD determination at 510 nm using a micro plate reader (Enspire, Perkin Elmer, USA). Using the seven absorbance measurements [time zero, (Tz), control growth, (C), and test growth in the presence of drug at the five concentration levels (Ti)], the percentage growth was calculated at each of the drug concentrations levels. Percentage growth inhibition was calculated as: [(Ti-Tz)/(C-Tz)] x 100 for concentrations for which Ti>/=Tz , [(Ti-Tz)/Tz] x 100 for concentrations for which Ti<Tz. Growth inhibition of 50 % (GI_{50}) was calculated from [(Ti-Tz)/(C-Tz)] x 100 = 50, which is the drug concentration resulting in a 50% reduction in the net protein increase (as measured by SRB staining) in control cells during the drug incubation.

4.4.3 Cell cycle analysis

Flow cytometric analysis (FACS) was performed to evaluate the distribution of the cells through the cell-cycle phases. MCF-7 cells, breast cancer cells were incubated for 48 h with compounds **16** and **27** at concentrations of 50 and 100 nM. Untreated and treated cells were harvested, washed with phosphate-buffered saline (PBS), fixed in ice-cold 70% ethanol, and stained with propidium iodide (Sigma–Aldrich). Cell-cycle analysis was performed by flow cytometry (Becton Dickinson FACS Caliber instrument) [38].

4.4.4 Western blot analysis

After treatment with test compounds **16** and **27** at 50, 100 nM concentrations for 48 h. Protein was isolated with RIPA (radioimmunoprecipitation assay) buffer. Protein (50 µg per lane)was applied in 10 % SDS-PAGE (Sodium dodecyl sulfate Polyacrylamide gel electrophoresis). After electrophoresis, the protein was transferred to a polyvinylidine difluoride (PVDF) membrane (Thermo Scientific Inc.) and blocked with BSA (bovine serum albumin).The membrane was washed with TBST for 5 min, then primary antibody was added. After 24 h, the membrane was incubated with the corresponding horseradish peroxidase labeled secondary antibody and incubated for another 1 h. Membranes were washed with TBST three times for 15 min and the protein blots were visualized with chemiluminescence reagent (Thermo ScientificInc.). Images were captured by using the chemiluminescence (vilberlourmat) [39].

4.4.5 Molecular Docking

The co-ordinates of the crystal structure were obtained from RCSB-Protein Data Bank. Required corrections to the protein were carried out by using Protein Preparation Wizard from Schrödinger package. Molecules were built using ChemBio3D Ultra 12.0 and geometries were optimized using molecular mechanics. All docking studies were performed by using Auto Dock 4.2 docking software [40] and the results were visualized through PyMOL [41].

4.4.6 Hoechst staining

The MCF-7 cells were seeded in 24-well plates at the density of $1X10^5$ cells per ml. After 24h, cells were incubated with test compounds **16** and **27** for 24 h. Cells treated with vehicle (DMSO) were included as controls for all experiment. After washing with PBS, cells were fixed with 4% para formaldehyde (PFA) in PBS for 10 min at 4 ºC and stained with Hoechst 33242 (life technologies) (2 µg/mL) for 10 min at room temp. Cells were washed twice with PBS to remove the excess dye. Cells from each well were captured from randomly selected fields under fluorescence microscope (Nikon).

4.4.7 Measurement mitochondrial membrane potential

The MCF-7 cells were plated at $1X10^5$ cells/mL in 24-well culture plates and allowed to adhere overnight. Cells were treated with GI_{50} concentrations of the compounds **16** and **27** for 24 h. After washing twice with PBS, cells were incubated with Rhodamine 123 (sigma Aldrich) (5 µg/ml) for 30 min in the dark at 37 ºC and cells were washed twice with PBS to remove the excess dye. The decrease in intensity of fluorescence because of mitochondrial membrane potential loss was analyzed using fluorescence microscope (Nikon).

4.4.8 Measurement of reactive oxygen species level

The MCF-7 cells were plated at $1X10^5$ cells /mL in 24-well culture plates and allowed to adhere for overnight. Cells were treated with compounds **16** and **27** for 24 h, washed with PBS and fixed with 4 % para formaldehyde. Cells were exposed with Carboxy-DCFDA dye (life technologies) (10 µM/mL) for 30 min in the dark at room temp and washed with PBS to remove the excess dye. The increase in intensity of fluorescence because of generation of reactive oxygen species was analyzed using fluorescence microscope (Nikon).

4.4.9 Annexin staining assay for apoptosis

MCF-7 (1×10^6) cells were seeded in six-well plates and allowed to grow overnight. The medium was then replaced with complete medium containing compounds **16** and **27** at concentrations of 50 and 100 nM concentrations. After 48 h of drug treatment, cells from the supernatant and adherent monolayer cells were harvested by trypsinization, washed with PBS at 5000 rpm. Then the cells were stained with Annexin V/FITC and propidium iodide using the Annexin-V-FITC apoptosis detection kit (Sigma aldrich).Flow cytometry was performed for this study as described earlier [42].

Acknowledgement

The authors V.G.R, B.P. and A.P.R. acknowledge the Council of Scientific and Industrial Research (CSIR), New Delhi (India) for the financial support under the 12th Five Year Plan project “Affordable Cancer Therapeutics (ACT)” (CSC0301). This project was also supported by King Saud University, Deanship of Scientific Research, Research Chair.

References

[1] M. Hall, G. Peters, Genetic alterations of cyclins, cyclin dependent kinases and Cdk inhibitors in human cancer, AdV. Cancer Res. 68 (1996) 67–108.

[2] S. van den Heuvel, Ed Harlow, Distinct roles for cyclin-dependent kinases in cell cycle control, Science. 262 (1993) 2050–2054.

[3] M. Malumbres, M. Barbacid, Milestones in cell division: To cycle or not to cycle: a critical decision in cancer, Nat. ReV. Cancer. 1 (2001) 222–231.

[4] J. Cicenas, M. Valius, The CDK inhibitors in cancer research and therapy, J. Cancer Res. Clin. Oncol. 137 (2011) 1409–1418.

[5] D.O. Morgan, Cyclin-dependent kinases: engines, clocks, and microprocessors, Annu.ReV. Cell DeV. Biol. 13 (1997) 261-291.

[6] Sherr CJ, Cancer cell cycles, Science. 274 (1996) 1672-1677.

[7] M. Malumbres, M. Barbacid, Cell cycle, CDKs and cancer: a changing paradigm, Nat. Rev. 9 (2009) 153–166.

[8] Th'ng JP. et al. The FT210 cell line is a mouse G2 phase mutant with a temperature sensitive CDC2 gene product, Cell. 63 (1990) 313–324.

[9] J.E. Itzhaki, C.S. Gilbert, A.C. Porter, Construction by gene targeting in human cells of a 'conditional' CDC2 mutant that rereplicates its DNA, Nat. Genet. 15 (1997) 258–265.

[10] P. M. Fischer, A. Gianella-Borradori, Recent progress in the discovery and development of CDK inhibitors, Expert Opin.InVest. Drugs. 14 (2005) 457-477.

[11] C. Benson, S. Kaye, P. Workman, M. Garrett, M. Walton, J. de Bono, Clinical anti cancer drug development: targeting the cyclin dependent kinases, Br. J. Cancer. 92 (2005)7-12.

[12] A. Czarnik, Guest Editorial, Acc. Chem. Res. 29 (1996) 112-113.

[13] G. Traquandi, M. Ciomei, D. Ballinari, E. Casale, N. Colombo, V. Croci, F. Fiorentini, A. Isacchi, A. Longo, C. Mercurio, A. Panzeri, W. Pastori, P. Pevarello, D. Volpi, P. Roussel, A. Vulpetti and M.G. Brasca, Identification of potent pyrazolo[4,3-h]quinazoline-3-carboxamides as multi-cyclin-dependent kinase inhibitors, J. Med. Chem. 53 (2010) 2171–2187.

[14] A.M. Vijesha, A.M. Isloor, S. Telkar, S.K. Peethambar, S. Rai, N. Isloor, Synthesis, characterization and antimicrobial studies of some new pyrazole incorporated imidazole derivatives, Eur. J. Med. Chem. 46 (2011) 3531-3536.

[15] Chang-Ji Zheng, Li-Li Xu, Liang-Peng Sun, Jing Miao, Hu-Ri Piao, Synthesis and antibacterial activity of novel 1,3-diphenyl-1H-pyrazoles functionalized with phenylalanine-derived rhodanines, Eur. J. Med. Chem. 58 (2012) 112-116.

[16] R.B. Pathaka, P.T. Chovatia, H.H. Parekh, Synthesis, antitubercular and antimicrobial evaluation of 3-(4-chlorophenyl)-4-substituted pyrazole derivatives, Bioorganic & Medicinal Chemistry Letters. 22 (2012) 5129–5133.

[17] D. Dias, B.S. Pacheco, W. Cunico, L. Pizzuti, C.M. Pereira, Recent advances on the green synthesis and antioxidant activities of pyrazoles, Mini Rev Med Chem. 14 (2015) 1078-1092.

[18] P.D. Sauzem, P. Machado, M. A. Rubin, G.S. Sant'Anna, H.B. Faber, A.H. de Souza, C.F. Mello, P. Beck, R.A. Burrow, H.G. Bonacorso, N. Zanatta, M.A.P. Martins, Design and microwave-assisted synthesis of 5-trifluoromethyl-4,5-dihydro-1H-pyrazoles: novel agents with analgesic and anti-inflammatory properties, Eur. J. Med. Chem. 43 (2008) 1237-1247.

[19] A.H. Kategaonkar, P.V. Shinde, A.H. Kategaonkar, S.K. Pasale, B.B. Shingate and M.S. Shingare, Synthesis and biological evaluation of new 2-chloro-3-((4-phenyl-1H-1,2,3-triazol-1-yl)methyl)quinoline derivatives via click chemistry approach, Eur. J. Med. Chem. 45 (2010) 3142–3146.

[20] Y.-C. Duan, Y.-C. Ma, E. Zhang, X.-J. Shi, M.-M. Wang, X.-W.Ye and H.-M. Liu, Design and synthesis of novel 1,2,3-triazole-dithiocarbamate hybrids as potential anticancer agents, Eur. J. Med. Chem. 62 (2013) 11–19.

[21] T.S. Reddy, H. Kulhari, V.G. Reddy, V. Bansal, A. Kamal, R. Shukla, Design, synthesis and biological evaluation of 1,3-diphenyl-1H-pyrazole derivatives containing benzimidazole skeleton as potential anticancer and apoptosis inducing agents, Eur. J. Med. Chem. 101 (2015) 790-805.

[22] T.S. Reddy, H. Kulhari, V.G. Reddy, A.V. Subba Rao, V. Bansal, A. Kamal and R. Shukla, Synthesis and biological evaluation of pyrazolo–triazole hybrids as cytotoxic and apoptosis inducing agents, Org. Biomol. Chem. 13 (2015) 10136-10149.

[23] T.S. Reddy, V.G. Reddy, H. Kulhari, R. Shukla, A. Kamal, V. Bansal, Synthesis of (Z)-1-(1,3-diphenyl-1H-pyrazol-4-yl)-3-(phenylamino)prop-2-en-1-one derivatives as potential anticancer and apoptosis inducing agents, Eur. J. Med. Chem. 117 (2016) 157-166.

[24] O. Prakash, K. Pannu and A. Kumar, Synthesis of Some New 2-(3-Aryl-1-phenyl-4-pyrazolyl)-benzoxazoles Using Hypervalent Iodine Mediated Oxidative Cyclization of Schiff's Bases, Molecules. 11 (2006), 43–48.

[25] K.T. Chan, F.Y. Meng, Q. Li, C.Y. Ho, T.S. Lam, Y. To, W.H. Lee, M. Li, K.H. Chu and M. Toh, Cucurbitacin B induces apoptosis and S phase cell cycle arrest in BEL-7402 human hepatocellular carcinoma cells and is effective via oral administration, Cancer Lett. 294 (2010) 118-124.

[26] J.K. Shen, H.P. Du, M. Yang, Y.G. Wang and J. Jin, Casticin induces leukemic cell deaththrough apoptosis and mitotic catastrophe, Ann. Hematol. 88 (2009) 743-752.

[27] M. Blank, Y. Shiloh, Programs for Cell Death: Apoptosis is Only One Way to Go, Cell Cycle. 6 (2007) 686-695.

[28] (a) C.J. Sherr, Science. 274 (1996) 1672-1677; (b) C.J. Sherr, Cancer Res. 60 (2000) 3689-3695; (c) J. Pines, Adv. Cancer Res. 66 (1995) 181-212; (d) C.J. Sherr, J.M.

Roberts, Genes Dev. 13 (1999) 1501-1512; (e) N. Dyson, Genes Dev. 12 (1998) 2245-2262.

[29] I. Neganova, K. Tilgner, A. Buskin, I. Paraskevopoulou, SP Atkinson, D. Peberdy, JF Passos and M. Lako, CDK1 plays an important role in the maintenance of pluripotency and genomic stability in human pluripotent stem cells, Cell Death Dis. 5 (2014) e1508. http://dx.doi.org/10.1038/cddis.2014.464.

[30] J.M Enserink and R.D Kolodner, Review An overview of Cdk1-controlled targets and processes, Cell dev. 5 (2010) 11.

[31] N.R. Brown, S. Korolchuk, M.P. Martin, W.A. Stanley, R. Moukhametzianov, M.E.M. Noble, J.A. Endicott, Nature Communications, doi:10.1038/ncomms7769. 6 (2015).

[32] A. Kamal, B. Shaik, V. L. Nayak, B. Nagaraju, J. S. Kapure, M. S. Malik, T. B. Shaik and B. Prasad, Synthesis and biological evaluation of 1,2,3-triazole linked aminocombretastatin conjugates as mitochondrial mediated apoptosis inducers, Bioorg. Med. Chem. 22 (2014) 5155–5167.

[33] C. D. Fan, H. Su, J. Zhao, B. X. Zhao, S. L. Zhang and J. Y. Miao, A novel copper complex of salicylaldehyde pyrazole hydrazone induces apoptosis through up-regulating integrin β4 in H322 lung carcinoma cells, Eur. J. Med. Chem. 45 (2010) 1438–1446.

[34] A. H. Wyllie, lucocorticoid-induced thymocyte apoptosis is associated with endogenous endonuclease activation, Nature. 284 (1980) 555-556.

[35] R. D. Miao, Y. Han, L. Z. An, J. B. Yang and Q. Wang, Seleno-podophyllotoxin derivatives induce hepatoma SMMC-7721 cell apoptosis through Bax pathway, Cell Biol. Int. 32 (2008) 217–223.

[36] D. Trachootham, J. Alexandre and P. Huang, Targeting cancer cells by ROS-mediated mechanisms: a radical therapeutic approach?, Nat. Rev. Drug Discovery. 8 (2009) 579–591.

[37] N. M. Weir, K. Selvendiran, V. K. Kutala, L. Tong, S. Vishwanath, M. Rajaram, S. Tridandapani, S. Anant and P. Kuppusamy, Curcumin induces G2/M arrest and apoptosis in cisplatin-resistant human ovarian cancer cells by modulating akt and p38 mAPK, Cancer Biol. Ther. 6 (2007) 178–184.

[38] M. Szumilak, M. A. Szulawska, K. Koprowska, M. Stasiak, W. Lewgowd, A. Stanczak, M. Czyz, Synthesis and in vitro biological evaluation of new polyamine conjugates as potential anticancer drugs, Eur. J. Med. Chem. 45 (2010) 5744-5751.

[39] G. Morris, R. Huey, W. Lindstrom, M. Sanner, R. Belew, D. Goodsell, A. Olson, Autodock4 And Autodocktools4: Automated Docking With Selective Receptor Flexibility. J. Comput. Chem. 30 (2009) 2785-2791.

[40] G. Shafi, A. Munshi, T. N. Hasan, A. A. Alshatwi, A. Jyothy, D. K.Y. Lei. Induction of apoptosis in HeLa cells by chloroform fraction of seed extracts of Nigella sativa. Cancer Cell Int. 9 (2009) 1–8.

[41] W.L. Delano, The PyMOL Molecular Graphics System; DeLano Scientific: San Carlos, California, 2002.

[42] L.J. Browne, C. Gude, H. Rodriguez, R.E. Steele, A.J. Bhatnager, Fadrozole hydrochloride: a potent, selective, nonsteroidal inhibitor of aromatase for the treatment of estrogen-dependent disease, J. Med. Chem. 34 (1991) 725-736.

Figure/Scheme Captions

Scheme 1. General synthesis of compounds **8-35**. Reagents and conditions: (i) EtOH, 50–60 °C, 3 h; (ii) DMF, $POCl_3$, 50–60 °C, 5 h; (iii) $NaClO_2/NH_2SO_3$, 40–50 °C, 5 h; (iv) DMF, EDCI, HOBt, propargyl amine, 0 °C- rt, 12 h; (v) substituted benzylazides, $CuSO_4.5H_2O$, sodium ascorbate, *t*-BuOH/H_2O (1:1), rt, 12 h.

Table 1. Antiproliferative activity ($^aGI_{50}$ µM) of compounds **8-35.**

Fig. 1. Examples of chemical structures of CDK1 inhibitors.

Fig. 2. Cell cycle analysis of compounds **16** and **27** on MCF-7 cells. A: Control cells (MCF-7), B: Nocodazole (100 nM), C: 16 (50 nM), D: 16 (100 nM), E: 27 (50 nM) and F: 27 (100 nM).

Fig.3. Effect of **16** and **27** on CDK1 expression levels. MCF-7 cells were treated with compounds for 48 h at 50 and 100 nM concentrations. The cell lysates were collected and expression level of CDK1 was determined by western blot analysis. β-actin was used as a loading control.

Fig. 4. a) Surfaced binding of **16** in LZ9 binding pocket, b) Hydrogen bonding of **16** with Leu83, c) and d) binding pose of compound **16** and **2**7 respectively. Compounds **16** and **27** are shown in stick and coloured by the atom type (carbon: cyan; oxygen: red; hydrogen: white; nitrogen: blue; chlorine: green; fluorine: ice blue).

Fig. 5. Effect of compounds **16** and **27** on nuclear morphological changes of MCF-7 cells. A) Control, B) 50 nM (compound 16), C) 100 nM (compound 16), D) 50 nM (compound 27), E) 100 nM (compound 27).

Fig. 6. Compounds **16** and **27** induced loss of mitochondrial membrane potential (DΨm) in MCF-7 cells analyzed using Rhodamine 123 staining. Images were captured by a fluorescence microscope. A) Control, B) 50 nM (compound 16), C) 100 nM (compound 16) D) 50 nM (compound 27), E) 100 nM (compound 27).

Fig. 7. Effect of compounds **16** and **27** on the intracellular levels of ROS. MCF-7 cells were treated with compounds **16** and **27** for 24 h and stained with carboxy DCFDA. A) Control, B) 50 nM (compound 16), C) 100 nM (compound 16) D) 50 nM (compound 27), E) 100 nM (compound 27). Images were captured by a fluorescence microscope.

Fig. 8. Annexin V-FITC assay; Quadrants; Upper left (necrotic cells), Lower left (live cells), Lower right (early apoptotic cells) and Upper right (late apoptotic cells). A: Control cells (MCF-7), B: Nocodazole (100 nM), C: 16 (50 nM), D: 16 (100 nM), E: 27 (50 nM) and F: 27 (100 nM).

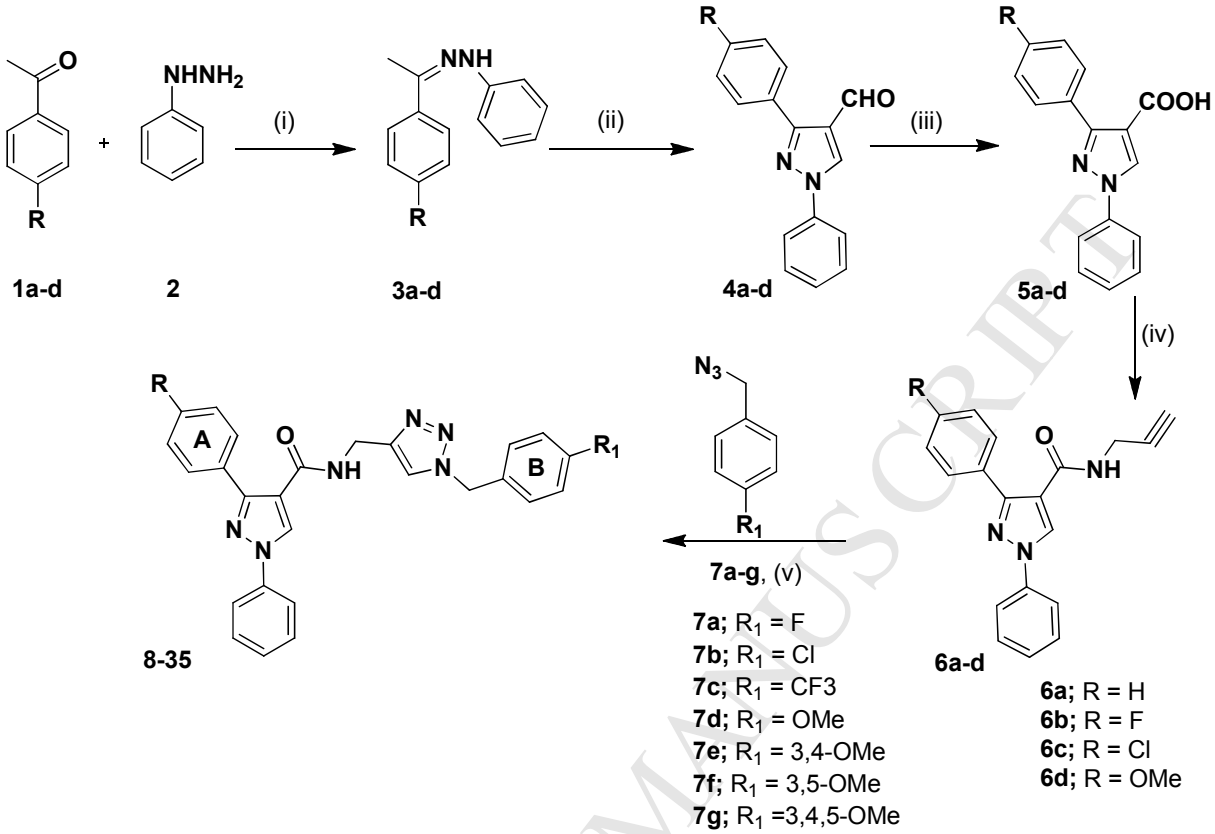

Scheme 1. General synthesis of compounds **8-35**. Reagents and conditions: (i) EtOH, 50–60 °C, 3 h; (ii) DMF, $POCl_3$, 50–60 °C, 5 h; (iii) $NaClO_2/NH_2SO_3$, 40–50 °C, 5 h; (iv) DMF, EDCI, HOBt, propargyl amine, 0 °C- rt, 12 h; (v) substituted benzylazides, $CuSO_4.5H_2O$, sodium ascorbate, *t*-BuOH/H_2O (1:1), rt, 12 h.

Table 1 Antiproliferative activity ([a]GI_{50} µM) of compounds **8-35.**

Compound	R	R_1	MIAPaCa-2[b]	MCF 7[c]	HeLa[d]
8	H	F	9.6±1.7	7.0±3.2	1.6±0.2
9	H	Cl	8.7±0.7	>100	0.6±0.1
10	H	CF_3	17.7±2.1	0.84±0.3	1.6±0.3
11	H	OMe	10.2±1.5	>100	6.9±1.3
12	H	3,4-OMe	8.2±1.2	12.6±0.7	10.8±1.2
13	H	3,5-OMe	0.19±0.02	2.4±0.4	12.2±0.7
14	H	3,4,5-OMe	1.0±0.03	>100	>100

15	F	F	14.3±1.1	55.3±9.4	1.2±0.9
16	**F**	**Cl**	**0.28±0.03**	**0.13±0.02**	**0.21±0.04**
17	F	CF_3	0.76±0.06	0.81±0.09	0.25±0.1
18	F	OMe	3.7±0.6	0.65±0.02	0.87±0.02
19	F	3,4-OMe	>100	>100	0.2±0.03
20	F	3,5-OMe	0.19±0.06	2.5±0.9	0.36±0.09
21	F	3,4,5-OMe	5.2±0.6	4.3±2.0	2.1±0.02
22	Cl	F	1.99±0.4	0.57±0.03	2.8±0.1
23	Cl	Cl	0.41±0.01	28.8±4.9	0.47±0.2
24	Cl	CF_3	1.1±1.0	4.9±0.4	1.9±0.3
25	Cl	OMe	0.29±0.1	8.0±0.6	1.4±0.2
26	Cl	3,4-OMe	9.4±2.4	>100	0.2±0.03
27	**Cl**	**3,5-OMe**	**0.34±0.02**	**0.15±0.02**	**0.73±0.04**
28	Cl	3,4,5-OMe	3.5±0.4	2.5±1.1	0.1±0.02
29	OMe	F	24.1±0.8	0.46±0.07	0.5±0.01
30	OMe	Cl	26.3±5.2	2.9±1.7	6.4±1.1
31	OMe	CF_3	>100	>100	6.2±5.4
32	OMe	OMe	2.5±0.2	22.9±3.9	0.45±0.2
33	OMe	3,4-OMe	16.3±2.8	>100	0.8±0.02
34	OMe	3,5-OMe	5.8±1.6	0.7±0.01	12.4±1.5
35	OMe	3,4,5-OMe	31.6±1.1	7.6±1.1	1.7±0.2
	Nocodazole		0.95 ± 0.013	0.94±0.02	0.81±0.01

[a]50% Growth inhibition and the values are mean of three independent experiments. [b]Pancreatic cancer, [c]Breast cancer and [d]Cervix cancer.

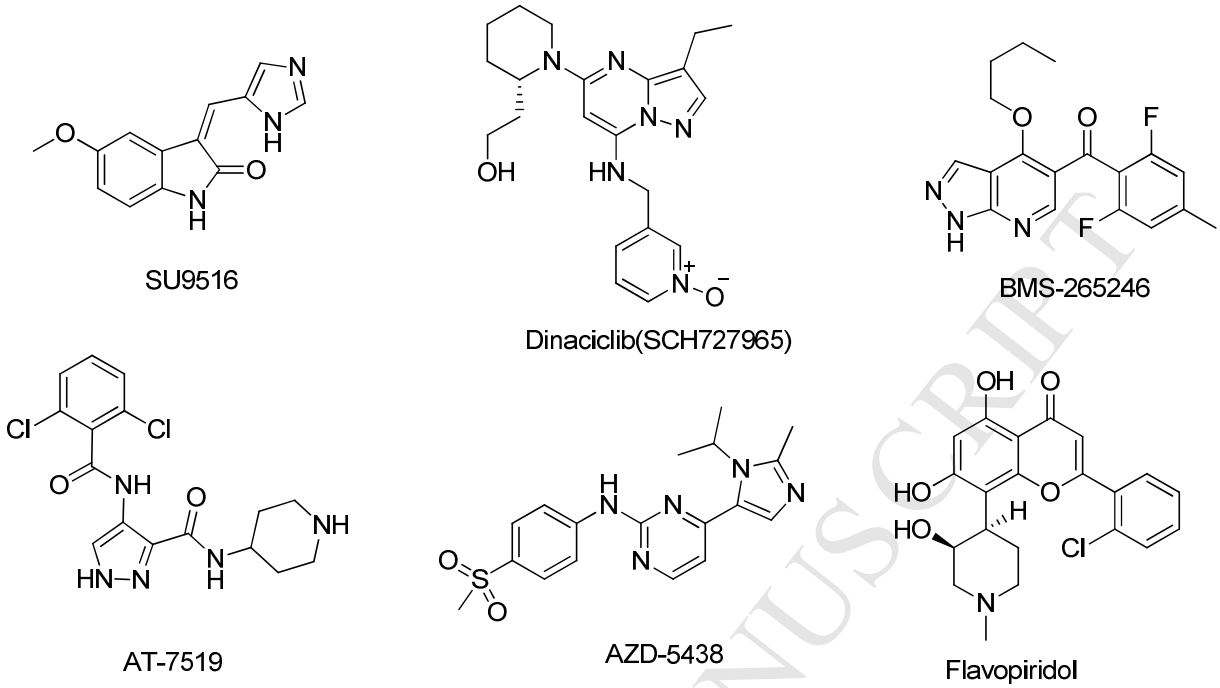

Fig. 1. Examples of chemical structures of CDK1 inhibitors.

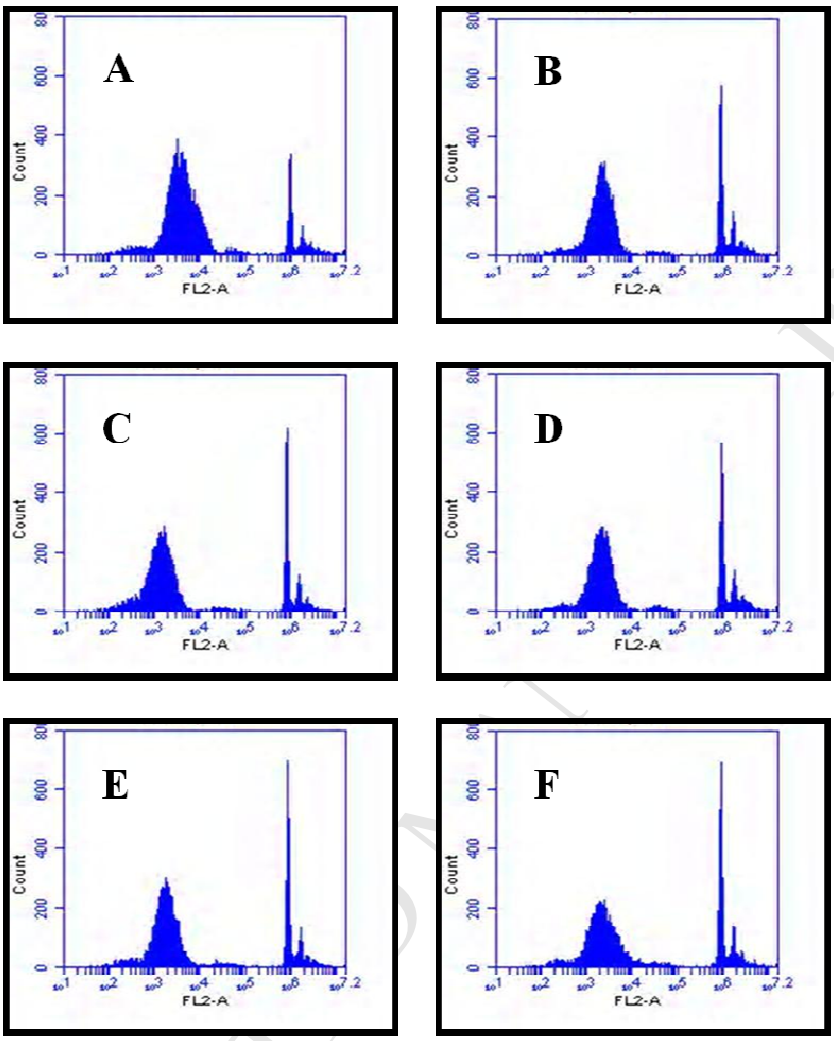

Fig. 2. Cell cycle analysis of compounds **16** and **27** on MCF-7 cells. A: Control cells (MCF-7), B: Nocodazole (100 nM), C: 16 (50 nM), D: 16 (100 nM), E: 27 (50 nM) and F: 27 (100 nM).

Sample	Sub G1 %	G0/G1 %	S %	G2/M %
A: Control	0.33	78.60	2.26	18.05
B: Nocodazole (100 nM)	0.45	65.27	1.42	32.14
C: 15 (50 nM)	0.70	66.85	1.15	29.58
D: 15 (100 nM)	0.41	64.17	1.64	32.54
E: 26 (50 nM)	0.43	64.57	1.57	32.26
F: 26 (100 nM)	0.45	61.49	1.73	34.96

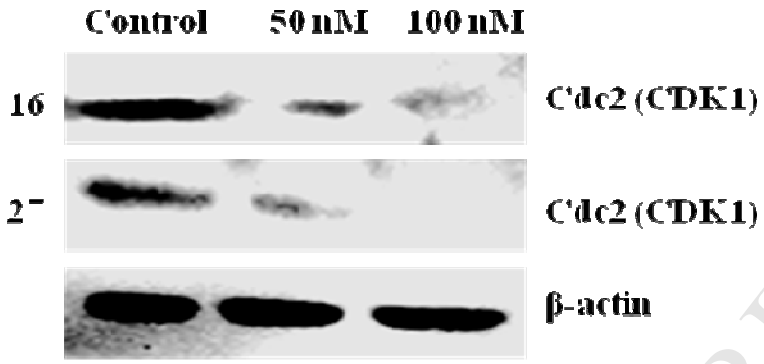

Fig.3. Effect of **16** and **27** on CDK1 expression levels. MCF-7 cells were treated with compounds for 48 h at 50 and 100 nM concentrations. The cell lysates were collected and expression level of CDK1 was determined by western blot analysis. β-actin was used as a loading control.

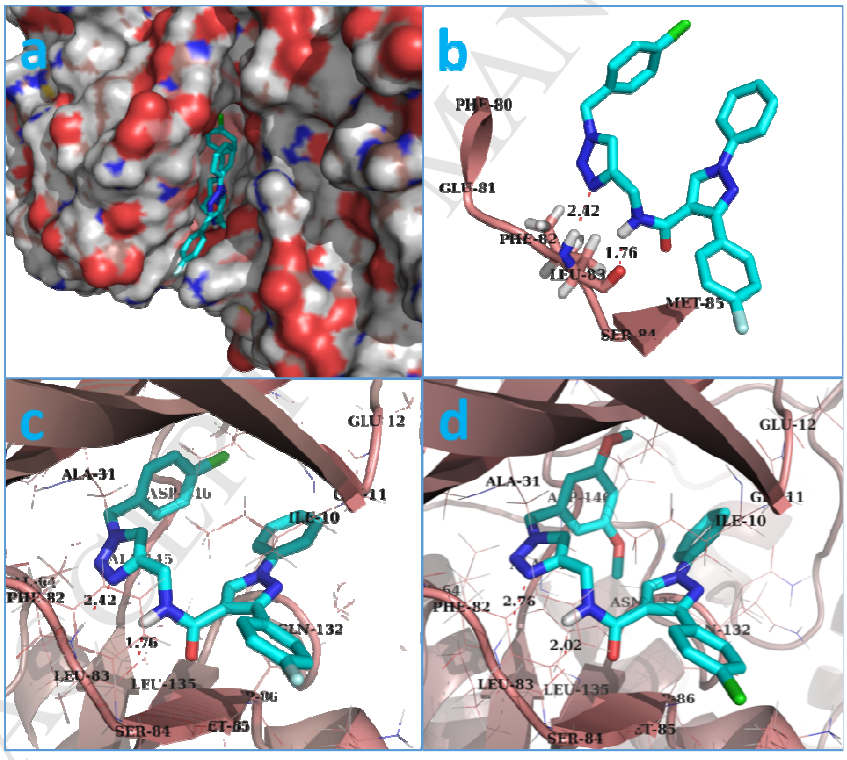

Fig. 4. a) Surfaced binding of **16** in LZ9 binding pocket, b) Hydrogen bonding of **16** with Leu83, c) and d) binding pose of compound **16** and **27** respectively. Compounds **16** and **27** are shown in stick and coloured by the atom type (carbon: cyan; oxygen: red; hydrogen: white; nitrogen: blue; chlorine: green; fluorine: ice blue).

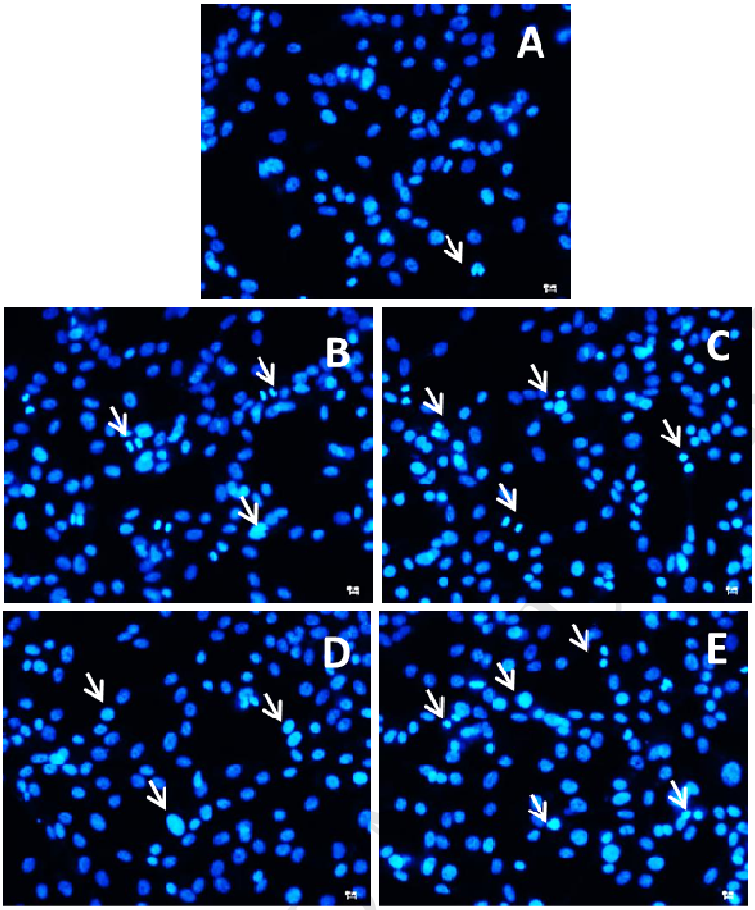

Fig. 5. Effect of compounds **16** and **27** on nuclear morphological changes of MCF-7 cells. A) Control, B) 50 nM (compound 16), C) 100 nM (compound 16), D) 50 nM (compound 27), E) 100 nM (compound 27).

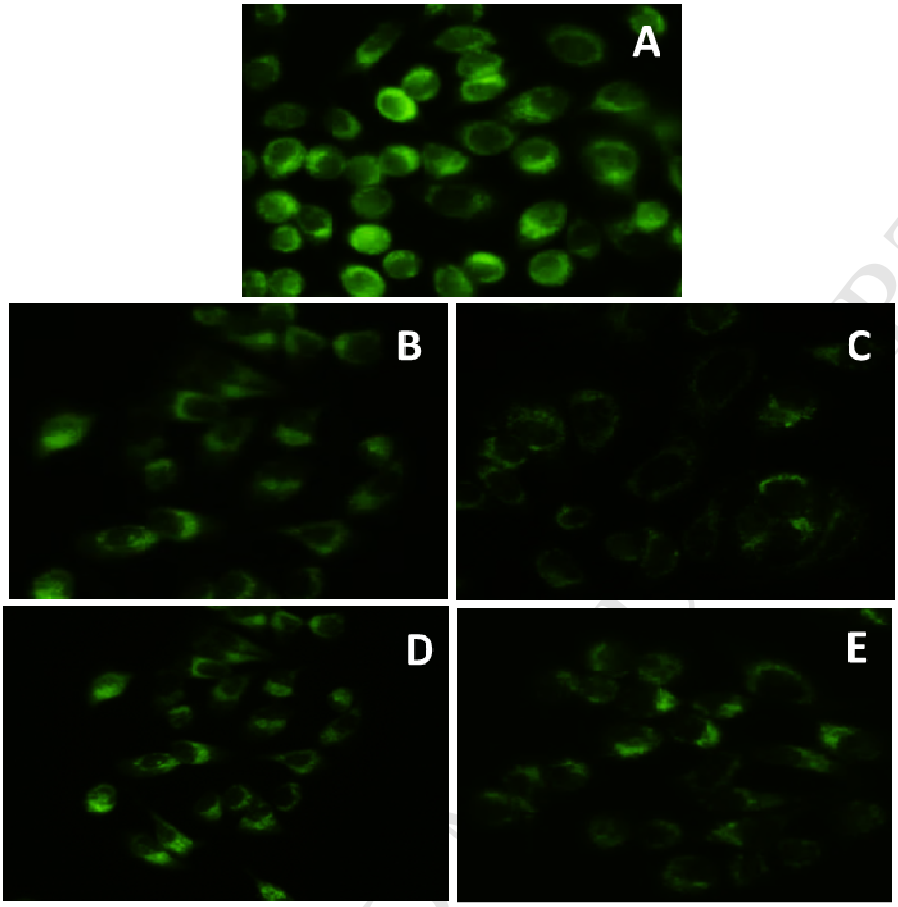

Fig. 6. Compounds **16**and **27**induced loss of mitochondrial membrane potential (DΨm) in MCF-7 cells analyzed using Rhodamine 123 staining.Images were captured by a fluorescence microscope. A) Control, B) 50 nM (compound 16), C) 100 nM (compound 16) D) 50 nM (compound 27), E) 100 nM (compound 27).

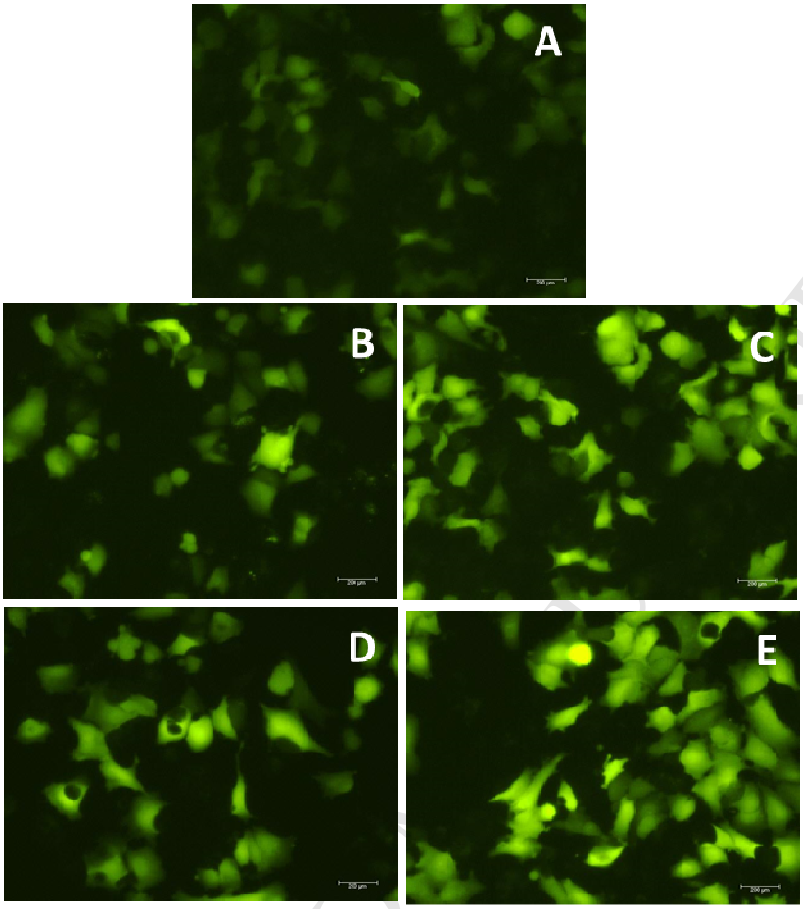

Fig. 7. Effect of compounds **16** and **27** on the intracellular levels of ROS. MCF-7 cells were treated with compounds **16** and **27** for 24 h and stained with carboxy DCFDA. A) Control, B) 50 nM (compound 16), C) 100 nM (compound 16) D) 50 nM (compound 27), E) 100 nM (compound 27). Images were captured by a fluorescence microscope.

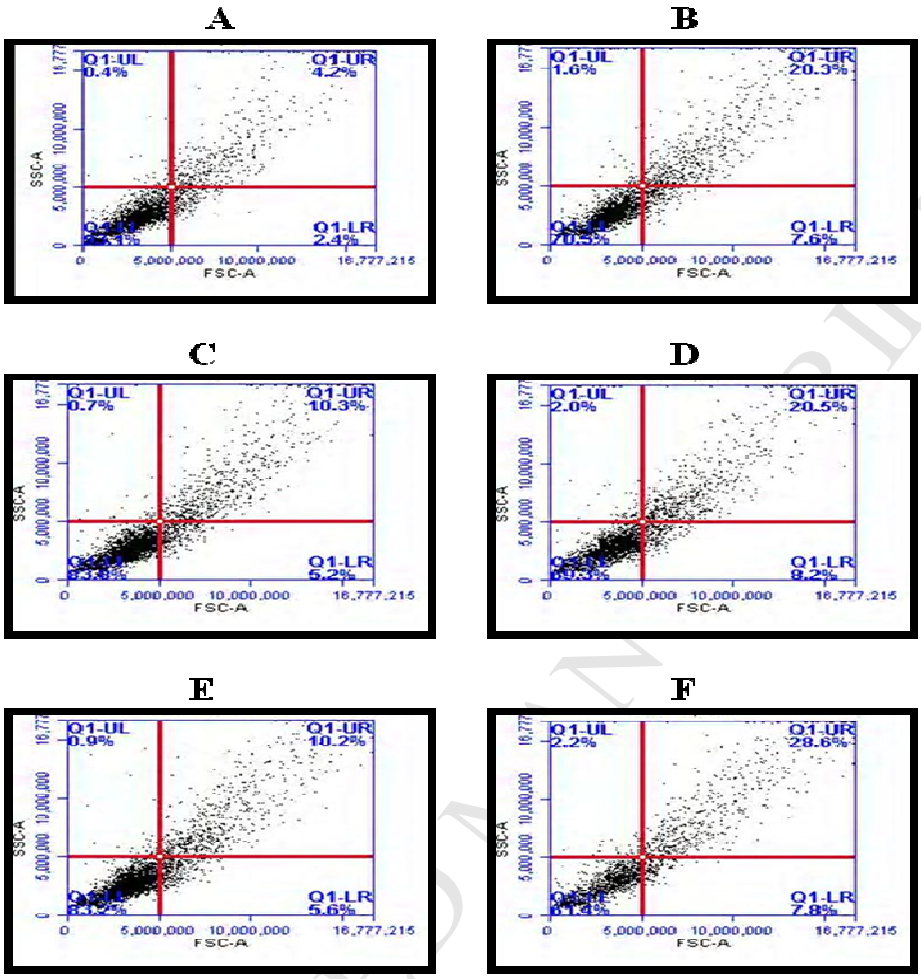

Fig. 8. Annexin V-FITC assay; Quadrants; Upper left (necrotic cells), Lower left (live cells), Lower right (early apoptotic cells) and Upper right (late apoptotic cells). A: Control cells (MCF-7), B: Nocodazole (100 nM), C: 16 (50 nM), D: 16 (100 nM), E: 27 (50 nM) and F: 27 (100 nM).

Sample	UL %	UR %	LL%	LR %
A: Control	0.42	4.16	93.05	2.37
B: Nocodazole (100nM)	1.62	20.29	70.48	7.61
C: 16 (50nM)	0.68	10.31	83.78	5.23
D: 16 (100nM)	2.02	20.48	69.34	8.17
E: 27 (50nM)	0.95	10.22	83.22	5.61
F: 27 (100nM)	2.18	28.64	61.37	7.81

Research Highlights

1). **28** derivatives (**8**-**35**) were synthesized and tested for their antiproliferative activity.

2). Compounds **16** and **27** showed significant cytotoxicity with GI_{50} 0.13 to 0.7 µM.

3). Compounds (**16** and **27**) induces cell cycle arrest in the G2/M phase.

4). Western blot analysis showed reduction of CDK1 expression levels in MCF-7 cell line.

5). Compounds (**16** and **27**) can be considered as interesting lead molecules for further development of more potent anticancer agents against breast cancer cells.